The official journal of the Japan Atherosclerosis Society and
the Asian Pacific Society of Atherosclerosis and Vascular Diseases

Original Article

J Atheroscler Thromb, 2020; 27: 71-99. http://doi.org/10.5551/jat.47704

DNA Methylation Analysis Identifies Differentially Methylated Sites Associated with Early-Onset Intracranial Atherosclerotic Stenosis

Xin-Wei He[1,2], Ying Zhao[1,2], Yan-Hui Shi[1,2], Rong Zhao[1,2], Yi-Sheng Liu[1,2], Yue Hu[1,2], Mei-Ting Zhuang[1,2], Yi-Lan Wu[1,2], Ge-Fei Li[1,2], Jia-Wen Yin[1,2], Guo-Hong Cui[1,2] and Jian-Ren Liu[1,2]

Xin-Wei He, Ying Zhao, Yan-Hui Shi and Rong Zhao contributed equally to this work.
Guo-Hong Cui and Jian-Ren Liu are joint senior authors.

[1]Department of Neurology, Shanghai Ninth People's Hospital, Shanghai Jiao Tong University School of Medicine, Shanghai, China
[2]Clinical Research Center, Shanghai Jiao Tong University School of Medicine, Shanghai, China

Aim: Studies have suggested that genetic and environmental factors do not account for all risks and mechanisms of intracranial atherosclerotic stenosis (ICAS). DNA methylation may play a role in the progression of ICAS.

Methods: DNA methylation profiles of peripheral blood leucocytes from 7 patients with early-onset ICAS and 7 perfectly matched controls were interrogated for the first time using the Illumina Infinium Human MethylationEPIC BeadChip. Afterward, functional analysis for differentially methylated genes was conducted. In addition, pyrosequencing verification was performed in an independent cohort comprising 21 patients with early-onset ICAS and 21 age- and gender-matched controls.

Results: A total of 318 cytosine-phosphate-guanine sites were found to be differentially methylated based on the established standards. Functional analysis annotated differentially methylated sites to atherosclerosis-related processes and pathways, such as the negative regulation of hydrolase activity (GO 0051346), type II diabetes mellitus (KEGG hsa04930), and the insulin signaling pathway (KEGG hsa04910). In addition, a differentially methylated site was also validated, cg22443212 in gene Rnf213, which showed significant hypermethylation in patients with early-onset ICAS compared with controls 59.56% (49.77%, 88.55%) vs. 44.65% (25.07%, 53.21%), respectively; $P=0.010$). Receiver operating characteristic curve analysis showed that the area under the curve value of cg22443212 was 0.744 (95% confidence interval, 0.586–0.866; $P=0.002$).

Conclusions: We revealed that altered DNA methylation may play a role in the occurrence and development of ICAS. These results provided new epigenetic insights into ICAS.

Key words: Intracranial atherosclerotic stenosis, Epigenetics, DNA methylation, Ring finger protein 213

Introduction

Intracranial atherosclerotic stenosis (ICAS) is an important etiology of ischemic stroke and a leading cause of recurrent stroke[1]. Numerous studies have confirmed the racial differences in ICAS, and individuals of Asian, African, and Hispanic ancestry are at higher risk of ICAS[2,3]. One favored hypothesis is that not only inherited susceptibility but also environmental exposure plays a critical role in the pathogenesis of ICAS. However, despite intensive efforts at large genome-wide association studies and epidemiological studies, attempts to clearly identify all risks and mechanisms have been relatively disappointing.

Aberrant epigenetic modifications may bridge the environmental and genetic factors and thus lead to certain pathological consequences. DNA methylation, a stable and widely studied epigenetic event, is a pro-

Address for correspondence: Jian-Ren Liu, Department of Neurology, Shanghai Ninth People's Hospital, Shanghai Jiao Tong University School of Medicine, Shanghai, China E-mail: liujr021@sjtu.edu.cn

Received: October 21, 2018 Accepted for publication: April 2, 2019

cess by which a methyl group is added to a nucleotide, usually cytosine nucleotides, in the presence of cytosine-phosphate-guanine (CpG)[4]. DNA methylation can affect gene expression and chromatin organization[4], and alterations in DNA methylation patterns might play a role in the progression of certain diseases[4, 5].

Both the global methylation status of the genome and aberrant methylation in certain specific methylated loci have been studied in several atherosclerotic lesions from extracranial carotid, coronary, or ascending aorta arteries[6-8]. Furthermore, epigenome-wide association studies have linked peripheral blood cell DNA methylation profiles of specific loci to hyperlipidemia, hyperglycemia, and obesity, thus uncovering candidate circulating epigenetic markers of atherosclerosis[9-11].

The intracranial artery has been reported to have anatomically and physiologically distinct characteristics, such as the structure of the arterial walls and wall shear stress, compared with the extracranial carotid, coronary, or other systemic arteries[12-14]. Studies on methylation profiling in patients with ICAS are limited. Since it is difficult to obtain intracranial vascular tissue, methylation signatures from the circulation of patients with ICAS hold promise as potential biomarkers that might be useful in clinical practice.

Age-related functional impairments are critical factors contributing to the risk and development of ICAS[1, 15], and DNA methylation changes may be associated with the aging process[8, 15, 16]. Thus, in order to reduce the influences of age-related dysfunction on both DNA methylation and ICAS, we performed this study focusing only on subjects with early-onset ICAS.

Aim

For the first time, we used a genome-wide DNA methylation analysis (Illumina Infinium Human MethylationEPIC BeadChip, Illumina Inc., San Diego, CA, USA) combined with pyrosequencing approaches to identify novel DNA methylation sites in peripheral blood leucocytes from patients with early-onset ICAS compared with those from controls.

Materials and Methods

Ethics Statement

This study was approved by the Ethics Committee of Shanghai Ninth People's Hospital, Shanghai Jiao Tong University School of Medicine. All procedures were performed in accordance with the ethical guidelines of the 1975 Declaration of Helsinki. Written informed consent was obtained from all participants included in the study.

Study Subjects

The definition of early-onset ICAS is unspecific. In this study, we recruited patients aged younger than 60 years, according to several previously published studies on coronary artery or carotid atherosclerosis[17, 18].

At the stage of chip interrogation, we enrolled 7 patients with ICAS and 7 controls. To eliminate interference from gene methylation induced by other factors as much as possible, we carefully screened and selected a similarly matched control for each patient. The matching factors included age, gender, and history of smoking, drinking, hypertension, diabetes, dyslipidemia, and drug use. In the pyrosequencing verification, a precise pair-match might not be possible, because we had only a limited number of controls for selection. Thus, the matching factors included just age and gender. There were no significant differences between the two groups with regard to demographic and clinical features (**Supplementary Table 1**).

The following inclusion criteria were applied: age ≤ 60 years and intracranial artery atherosclerosis causing ≥ 50% stenosis in one or more major intracranial arteries[19]. In addition, the exclusion criteria were extracranial atherosclerosis with significant stenosis (≥ 50%), hemorrhagic stroke or moyamoya disease (MMD), severe coronary heart disease (CHD) or arrhythmia, hyperthyroidism or hypothyroidism, hematological disease, severe hepatic or renal insufficiency, a history of tumors, chronic inflammation, recent infection, or recent surgery.

Vascular Assessments

Intracranial arteries were assessed by at least one of the following examinations: magnetic resonance angiography (MRA), computed tomography angiography (CTA), or digital subtraction angiography (DSA). We assessed the intracranial artery segments, including the intracranial internal carotid artery, anterior cerebral artery, middle cerebral artery, posterior cerebral artery, intracranial vertebral artery, and basilar artery, and if there was a reduction of ≥ 50% in luminal diameter of any of these arterial segments[19]. The exact degree of stenosis was measured by comparing the diameter of the vessel at the site of stenosis (D stenosis) with the normal diameter of the vessel just distal to the stenosis (D distal) using the following formula: % stenosis = [1 − (D stenosis/D distal)] × 100%[19]. Two independent investigators blinded to the clinical information and results of the methylation assay read and verified all images.

Blood and Baseline Data Collection and Definition

Fasting blood samples were collected from the participants in the morning after an overnight fast. Blood specimens were collected in EDTA-treated tubes and then stored at −80℃ before being assayed. All samples were thawed only once prior to use. Blood biochemistry tests (e.g., fasting blood glucose and blood lipids) were performed at the clinical laboratory in the hospital.

The clinical and demographic characteristics of the enrolled participants, such as gender, age, smoking and drinking status, history of disease, and medication, were recorded. All patients underwent standardized diagnostic tests. Hypertension was defined as a mean systolic blood pressure >140 mmHg and/or a mean diastolic blood pressure >90 mmHg at two measurements, or a medical history of anti-hypertensive drugs. Diabetes mellitus was defined as fasting blood glucose >7.00 mmol/L or a medical history of glucose-lowering drugs. Dyslipidemia was defined as serum triglycerides ≥ 1.69 mmol/L, low-density lipoprotein cholesterol ≥ 3.41 mmol/L, or the use of lipid-lowering drugs. Smoking was defined as smoking at the time of stroke or had quit smoking within 1 year, and drinking was defined as >2 standard alcoholic beverages consumed per day.

DNA Extraction and Bisulfite Treatment

Genomic DNA (gDNA) was extracted from leucocytes from venous blood samples using a QIAamp DNA Mini Kit (Qiagen, Hilden, Germany). The purity and concentrations of DNA samples were determined using a NanoDrop 1000 Spectrophotometer and Qubit 3.0 Fluorometer (Thermo Fisher Scientific, Waltham, MA, USA). The gDNA samples were bisulfite converted using an EZ DNA Methylation Kit (ZYMO Research, Irvine, CA, USA).

Genome-Wide DNA Methylation Profiling

DNA methylation assessment was performed using the Infinium Human MethylationEPIC BeadChip (Illumina Inc.) to interrogate more than 850,000 CpG positions across the genome. The raw image intensities of the hybridized arrays were scanned using an iScan SQ scanner (Illumina). The obtained raw data were processed and standardized using GenomeStudio software 2011.1 (Illumina), and the background method was chosen as the normalization method. Methylation values were estimated as β-values that range between 0 (completely unmethylated) and 1 (completely methylated). The experimental process and technical validation were performed according to the manufacturer's instructions.

Differential Methylation Analysis

A *t*-test was used to compare methylation profile differences between the two groups. For quality control, the CpG sites with missing values or the detection of $P>0.05$ in more than 90% of specimens were eliminated.

Single CpG sites with an absolute value of DiffScore >13 and an absolute $\delta(\beta)$ >0.17 were considered differentially methylated loci. The DiffScore is a transformation of the *P*-value that provides directionality to the *P*-value based on the difference between the average signals in the patient group vs. the control group. The formula is as follows: DiffScore = 10^{*}sgn($\delta(\beta)$)*log10(P), $\delta(\beta)=\beta$(patients) − β(controls). For a *P*-value of 0.05, DiffScore = ± 13.

Gene Ontology (GO) and Kyoto Encyclopedia of Genes and Genomes (KEGG) Pathway Analyses

GO and KEGG analyses were applied to determine the roles of the differentially methylated genes.

The pathway data were extracted from two standard public pathway databases: KEGG (http://www.kegg.jp/kegg/pathway.html) and GO (www.geneontology.org). The GO terms and KEGG pathways were considered significantly enriched with unadjusted raw $P<0.05$ and ranged according to -log10(P) from the lowest to the highest.

Validation by Pyrosequencing

Pyrosequencing assays were performed to validate the results obtained from CpG methylation analysis. Briefly, bisulfite-treated DNA was used for polymerase chain reactions (PCRs) with biotinylated primers using a PyroMark PCR kit (Qiagen). In addition, the biotinylated amplicons were purified to the final PCR product using Streptavidin Sepharose beads. The PCR product was bound to Streptavidin Sepharose HP (Amersham Biosciences, Uppsala, Sweden), and the Sepharose beads containing the immobilized PCR product were purified, washed and denatured using denaturation solution, and rewashed using a Pyrosequencing Vacuum Prep Tool (Pyrosequencing, Qiagen) as recommended by the manufacturer. Pyrosequencing reactions and methylation quantification were carried out on a PSQ96 HS System (Pyrosequencing, Qiagen) using appropriate reagents and protocols. Sequencing controls were included in each run to ensure the fidelity of the measurements. The forward and reverse PCR primers (from 5′ to 3′) used were GTGTTTTAGGTTTGGTTAAGTTTAGTTT and ACCTTCAAAACAAACATACTCTT, and the sequencing primer (from 5′ to 3′) used was AGTTGTAGGAGTGGG.

Table 1. Baseline and clinical characteristics of the participants for DNA methylation beadchip

Characteristic	Patients (n=7)	Controls (n=7)	P value
Demographics			
Age (years)	54 (53, 56)	59 (55, 59)	0.535
Male (%)	6 (85.7)	6 (85.7)	1.000
Hypertension (%)	5 (71.4)	5 (71.4)	1.000
Diabetes mellitus (%)	1 (14.3)	1 (14.3)	1.000
Dyslipidaemia (%)	3 (42.9)	3 (42.9)	1.000
Smoking (%)	6 (85.7)	6 (85.7)	1.000
Drinking (%)	2 (28.6)	2 (28.6)	1.000
SBP (mmHg)	140 (115, 144)	150 (149, 157)	0.805
DBP (mmHg)	78 (78, 80)	88 (88, 91)	0.710
Laboratory parameters			
FBG (mmol/L)	6.30 (5.20, 8.90)	4.70 (4.25, 5.00)	0.149
TG (mmol/L)	1.71 (1.40, 3.07)	2.25 (1.50, 2.26)	0.535
TC (mmol/L)	3.90 (3.65, 4.54)	5.66 (5.57, 5.89)	0.259
HDL-C (mmol/L)	0.85 (0.80, 0.96)	1.34 (1.06, 1.37)	0.805
LDL-C (mmol/L)	2.82 (2.28, 3.26)	3.93 (3.82, 4.14)	0.097
Homocysteine (μmol/L)	15.70 (9.10, 19.00)	8.60 (8.15, 11.40)	0.945
Fibrinogen (g/L)	1.98 (1.66, 2.14)	2.33 (2.29, 2.57)	0.610
CRP (mg/L)	3.90 (3.40, 5.41)	3.30 (3.16, 3.30)	0.234
Urea nitrogen (mmol/L)	4.60 (4.50, 6.10)	6.60 (5.80, 6.65)	0.295
Uric acid (μmol/L)	286.0 (246.0, 300.0)	279.0 (268.0, 335.0)	0.234
Creatinine (μmol/L)	91.0 (75.3, 100.3)	88.0 (80.0, 99.0)	1.000

Continuous variables are expressed as the mean ± standard deviation or the median (interquartile range). Categorical values are presented as frequencies (percentages).
Abbreviations: SBP, systolic blood pressure; DBP, diastolic blood pressure; FBG, fasting blood glucose; TG, triglycerides; TC, total cholesterol; HDL-C, high-density lipoprotein cholesterol; LDL-C, low-density lipoprotein cholesterol; CRP, C-reactive protein.

Statistical Analysis

Data are presented as the mean ± standard deviation or median (interquartile range) for continuous variables and as count and percentage for categorical variables. The Shapiro–Wilk test was used to test variables for normal distribution. Continuous data were analyzed using a Student's t-test (normal distribution) or the Mann–Whitney U test (non-normal distribution). Categorical data were analyzed using Pearson's χ^2 test or Fisher's exact test. Receiver operating characteristic (ROC) curve analysis was used to determine diagnostic accuracy, and the cut-off point was calculated by maximizing the sensitivity according to the Youden index. Statistical analyses were performed using SPSS 18.0 software (SPSS Inc., Chicago, IL, USA) or MedCalc 12.5 (MedCalc Software, Ostend, Belgium). A P-value <0.05 was considered to indicate statistical significance.

Results

Identifying Differential DNA Methylation Sites

We compared genome-wide DNA methylation profiles between the 7 patients with ICAS and the 7 matched controls. The basic characteristics of these subjects are summarized in **Table 1**. There were no significant differences in terms of demographic data between the two groups.

A total of 866,091 CpG sites that passed the quality control procedure were analyzed in this study. The scatterplot shows a high correlation of methylation levels between patients and controls (**Fig. 1A**). Principal component analysis showed that the majority of patients and controls could be divided into two clusters (**Supplementary Fig. 1**). The Manhattan plot showed the distribution of possible differentially methylated CpG sites on each chromosome (**Supplementary Fig. 2**).

Three hundred and eighteen differentially methylated CpG sites, including 183 hypermethylated sites

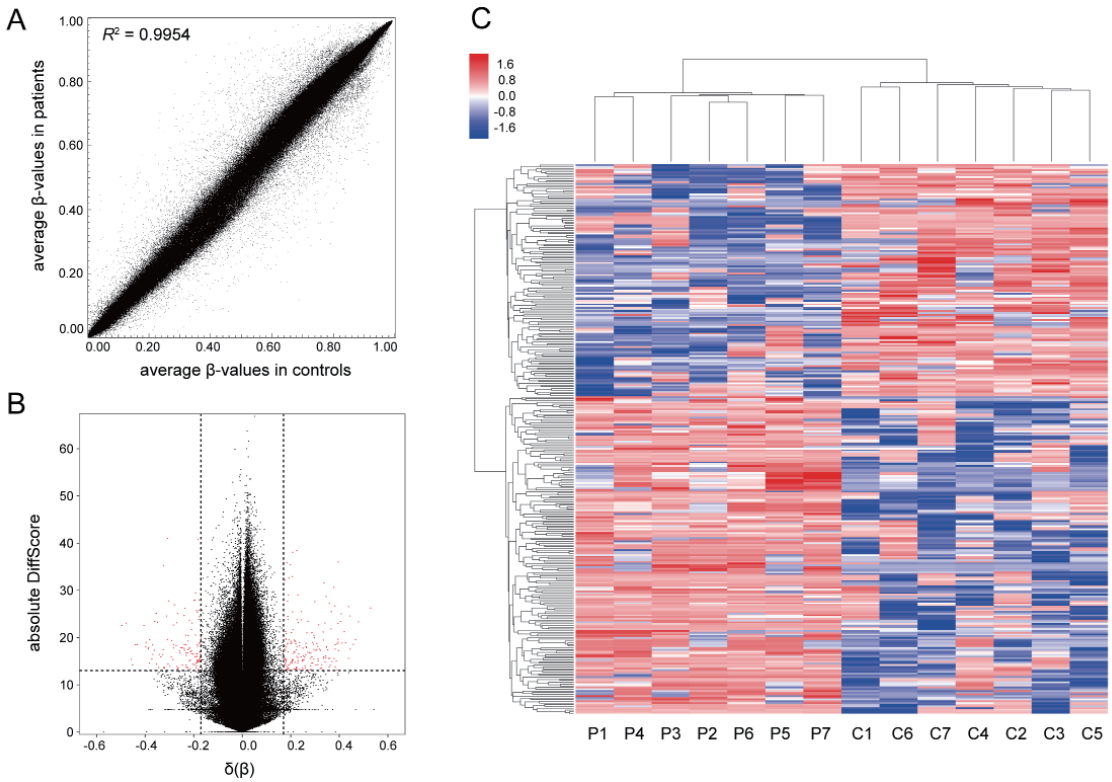

Fig. 1. Methylation profiles of patients with ICAS and controls

A: Scatterplots of probe intensities measuring the methylation level. X- and Y-axes represent the average β-values in subjects with ICAS and in controls, respectively. B: Volcano plots showing possible differentially methylated CpG sites. The X-axis represents the magnitude of the difference in signal intensity between the groups for each probe in the microarray, expressed as $\delta(\beta) = \beta(\text{patients}) - \beta(\text{controls})$. The Y-axis represents the absolute DiffScore, and DiffScore = 10*sgn($\delta(\beta)$)*log10(P). For a P-value of 0.05, DiffScore = ± 13. Significant differences (an absolute DiffScore > 13 and an absolute $\delta(\beta) > 0.17$) are shown in red. C: Hierarchical cluster analysis of differentially methylated CpG sites identified in this study. The red color in the heat map denotes hypermethylated loci and the blue color denotes hypomethylated loci.

and 135 hypomethylated sites, were identified in patients compared with controls, based on the established standards (**Supplementary Table 2; Fig. 1B**); of these, 114 sites were located in or around CpG islands (within 4 kilobases of a CpG island). In addition, cluster analysis for different methylation profiles was performed using two-way hierarchical clustering (**Fig. 1C**).

Functional Analysis

We then assigned the changed methylation sites to known gene regions. Altogether, we identified 168 differentially methylated genes (**Supplementary Table 3**). To identify common functional characteristics of the differentially methylated genes, GO analysis for biological process terms and KEGG pathway analysis were performed. The differentially enrichment of GO terms and KEGG pathways were identified by unadjusted P. In addition, convincing evidence suggested that methylated CpGs near transcription start sites (TSSs) can directly cause gene silencing or even activation[20, 21]. Thus, the genes in which differential methylation sites near the TSS (within 1500 bp) are located were also analyzed.

GO analysis for biological processes revealed that the top 4 terms are associated with inflammation-related biological processes (**Fig. 2A and Supplementary Table 4**). Additionally, GO analysis for genes of the different sites near TSSs also supported the enrichment results (**Fig. 2B and Supplementary Table 5**). In particular, the negative regulation of hydrolase activity (GO 0051346) was in the foremost findings in both GO analyses.

KEGG pathway analysis of differentially methylated genes revealed connections between the differentially methylated sites and the enrichment of glycometabolism-related pathways, that is, 3 of the top 5 pathways in the analysis for genes of all differentially meth-

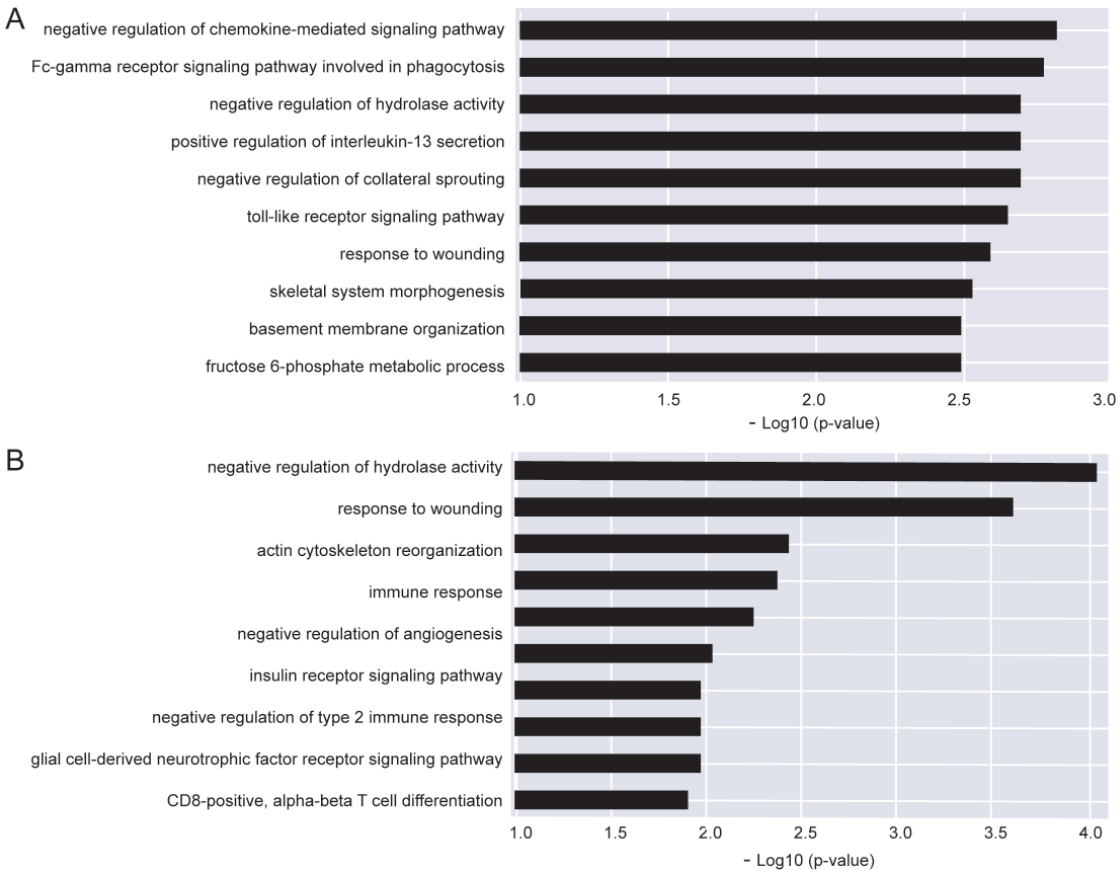

Fig. 2. Gene Ontology (GO) biological analysis of related genes that are associated with differentially methylated sites

The X-axis represents the *P*-value and the Y-axis represents the GO terms. A: For all differentially methylated sites. B: For differentially methylated sites near transcription start sites.

ylated sites and 4 of the top 5 pathways for genes of the different sites near TSSs (**Fig. 3A and Fig. 3B, and Supplementary Table 6 and Table 7**). In addition, type II diabetes mellitus (KEGG hsa04930) and the insulin signaling pathway (KEGG hsa04910) were in the top findings in both pathway analyses.

Validation by Pyrosequencing

Previous studies have reported that ring finger protein 213 (RNF213) is associated with intracranial vascular lesions[22, 23], and we identified a methylation site, cg22443212, in the gene body of RNF213 (*Rnf213*) that showed significant hypermethylation in patients in the chip interrogation assay [$\delta(\beta)=0.201$ and DiffScore=18.659]. Thus, to verify the differential methylation of cg22443212, pyrosequencing was performed in an independent cohort comprising 21 patients with early-onset ICAS and 21 age- and gender-matched controls (**Supplementary Table 1**). Pyrosequencing analysis showed significant hypermethylation of cg22443212 in patients with ICAS compared with controls [59.56% (49.77%, 88.55%) vs. 44.65% (25.07%, 53.21%); $P=0.010$; **Fig. 4A**], supporting the accuracy of the DNA methylation profile analysis results from the chip interrogation assay. Furthermore, the ROC curve analysis showed that the area under the curve value of cg22443212 that discriminated the presence of ICAS was 0.744 (95% confidence interval, 0.586–0.866; $P=0.002$; **Fig. 4B**), and by the Youden index, the optimal cut-off value for cg22443212 as a diagnostic marker of stroke was 44.65%, which yielded a sensitivity of 95.24% and a specificity of 52.38%.

Discussion

To the best of our knowledge, this is the first study to reveal differential DNA methylation in patients with early-onset ICAS compared with controls. A total of 318 CpG sites were found to be differentially methylated based on the established standards, suggesting an implication of methylation in

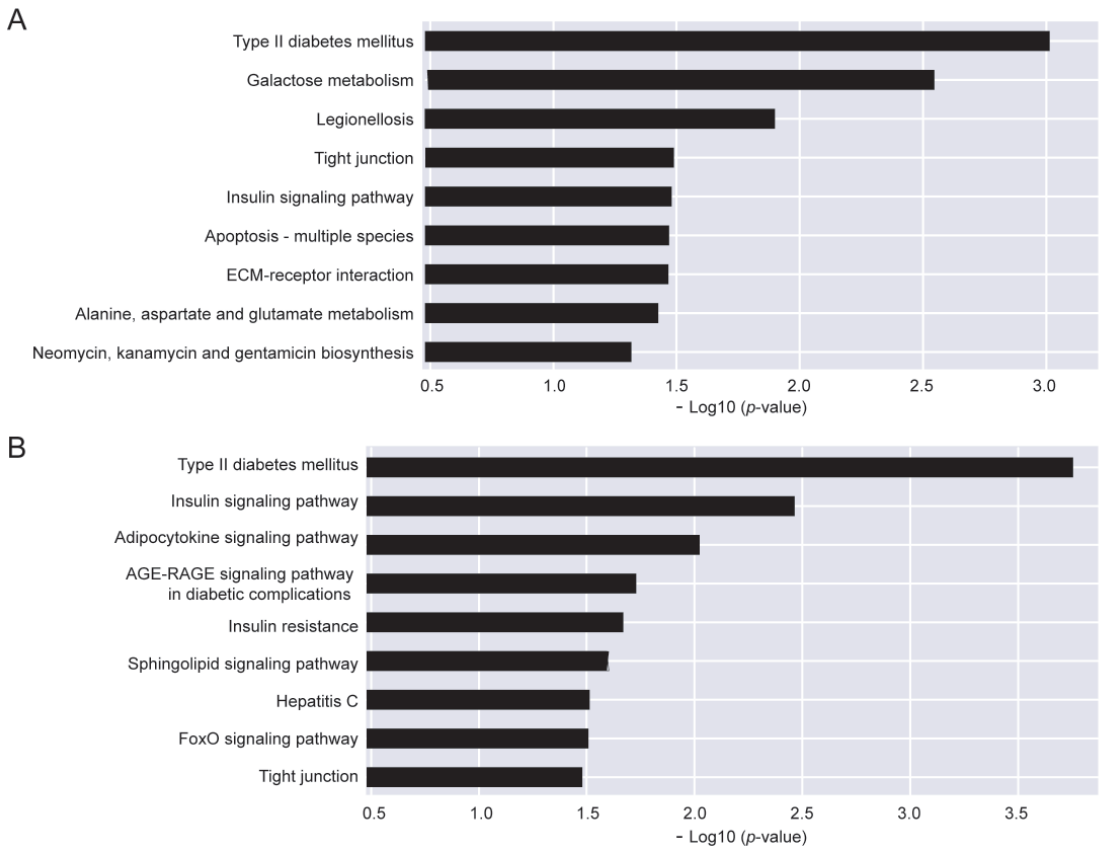

Fig. 3. Kyoto Encyclopedia of Genes and Genomes (KEGG) pathway analysis of related genes that are associated with differentially methylated sites

The X-axis represents the *P*-value and the Y-axis represents the pathways. A: For all differentially methylated sites. B: For differentially methylated sites near transcription start sites.

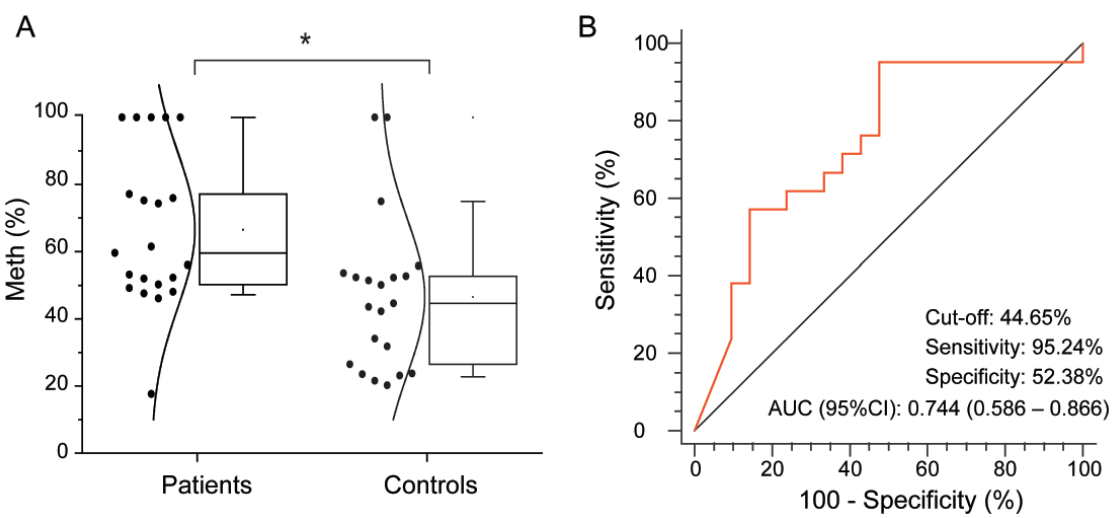

Fig. 4. Pyrosequencing assays validated the hypermethylation of cg22443212

A. Comparison of the methylation level of cg22443212 in patients with ICAS and controls. The black spots represent the actual value for each sample. In the box-and-whisker plots, the horizontal line in the middle of each box indicates the median value, the lower and upper ends of the box represent the 25th and 75th percentiles, respectively, and the peripheral whiskers represent the 10th and 90th percentiles. $^{*}P<0.05$. B. Receiver operating characteristic curve analysis for cg22443212 to discriminate patients with ICAS. The figure shows the best predictive value according to the Youden index. Abbreviations: AUC, area under the curve; 95% CI, 95% confidence interval.

ICAS. Functional analysis annotated differentially methylated sites to atherosclerosis-related processes. In addition, we also identified and validated a significantly hypermethylated site, cg22443212, in the gene *Rnf213* for the first time. The methylation level of cg22443212 showed significant diagnostic accuracy in discriminating patients from controls.

Indeed, there is a close connection between atherosclerosis and circulation, and peripheral blood leucocytes are ideal as they play vital roles in atherosclerosis[24, 25]. Accumulating evidence has illustrated the feasibility of DNA methylation profiling using peripheral blood to identify clinical correlations with surrogate markers of atherosclerosis in patients with atherosclerosis-related disease[26-28]. In addition, studies have reported that the methylation status of some sites in atherosclerotic plaques is similar to blood from patients with extracranial carotid, coronary, or aorta artery atherosclerosis[29, 30]. Moreover, animal studies have demonstrated that changes in the methylation level in peripheral blood and aortas of genetically atherosclerosis-prone mice precede the appearance of any histological sign of atherosclerosis[31]. Thus, we postulate that differential methylation in blood leucocytes may serve as a potential biomarker in clinical practice to monitor the disease and associated comorbidities.

Atherosclerosis is considered a chronic inflammatory condition of the vessel wall. In our GO analysis for biological processes of differentially methylated genes, we further revealed the connections between inflammation-related biological processes and ICAS. For instance, the negative regulation of hydrolase activity was found in the foremost terms. Hydrolases carry out important degradative reactions in the body, cleaving large molecules into fragments that are used as a source of energy or for the excretion of waste materials. Abnormal hydrolase activity is certain to influence metabolic processes. For instance, the gene *PRKCZ*, encoding protein kinase C ζ (PKCζ), is a gene in the pathway of negative regulation of hydrolase activity found in our KEGG analysis. Accumulating studies suggested important roles of PKCζ in the process of atherosclerosis, such as regulating not only endothelial apoptosis but also tumor necrosis factor-α -induced endothelial inflammation[32, 33], promoting monocyte adhesion by increased nuclear factor-κ B-dependent intercellular adhesion molecule 1 expression[33], and participating in upregulating the expression of ATP-binding cassette transporter protein family member A1 and promoting cholesterol efflux in THP-1 macrophage-derived foam cells[34].

In KEGG pathway analysis, we found that the identified differentially methylated sites tended to be located in genes functionally related to glycometabolism, that is, the type II diabetes mellitus and the insulin signaling pathway. It is well known that atherosclerosis is one of the most severe complications associated with type 2 diabetes mellitus. Atherosclerosis occurs earlier and with greater severity in patients with diabetes, suggesting that abnormal glucose metabolism significantly accelerates rates of atherosclerosis. Although information on the methylation regulation of genes involved in the pathophysiology of ICAS is scant, the methylation of glycometabolism-related genes in other atherosclerotic diseases has been reported preliminarily[12, 21, 22]. For instance, *GCK*, an encoded glucokinase that is a key enzyme of glucose phosphorylation, participates in the aforementioned pathways. A previous study has provided evidence that hypomethylation in the gene body of *GCK* was significantly associated with the risk of CHD[35]. The authors speculated that the decrease in GCK methylation in CHD cases may influence transcription and gene expression[35]. Additionally, literature has suggested that defects in the insulin signaling pathway result in insulin resistance and contribute to metabolic dysfunction and cardiovascular disease[34]. Recent studies have reported that the mechanism also involves methylation modification: high insulin levels reduce the methylation of leptin and adiponectin and induce the methylation of estrogen receptor α, resulting in atherosclerosis[34, 36].

Together, both biological processes and metabolic pathways of the genes of differentially methylated sites in our functional analysis are annotated to numerous atherosclerosis-related processes. Although particular DNA methylation studies of these processes have been limited up to now, methylation modification should represent an attractive molecular mechanism providing new insights into ICAS. Moreover, by comparing our results with other published methylation studies of atherosclerosis[28], we found that differences exist in both differentially methylated sites and functional analysis. These discrepancies highlight the differences in methylation involved in atherosclerosis between the intracranial artery and other systemic arteries. After all, different anatomical and physiological characteristics are known to exist[12-14]. Further studies are warranted to unravel the mechanisms involved in methylation regulation.

In this study, pyrosequencing analysis validated the methylation status of cg22443212, a locus in the gene body of *Rnf213*, showing hypermethylation in patients with ICAS compared with controls, which was consistent with the finding in the methylation BeadChip analysis.

RNF213 is a protein with two consecutive AAA^+ ATPase domains and one ring finger structure[37]. Previous studies have found that RNF213 is linked to a

variety of arterial wall development and remodeling processes and aberrant wall formation[22, 23], although the exact molecular mechanisms by which RNF213 regulates the aforementioned processes remain largely unknown. The relationships of RNF213 with known molecular pathways of the remodeling vasculature, such as noncanonical WNT/Ca^{2+}/NFAT signaling, have been revealed gradually[38]. In addition, recent reports also showed that RNF213 is associated with immune and inflammatory responses in these processes[39, 40]. Until now, no research on DNA methylation changes in *Rnf213* has been reported. Several genetic polymorphisms in this gene have been linked to intracranial vascular lesions, such as MMD[41, 42], non-MMD ICAS[42-44], and cerebral aneurysms[45]. Interestingly, accumulating studies suggested that *Rnf213* variants differ between early- and late-onset disorders[41, 46], which shows that phenotypic heterogeneity in patients cannot be explained solely by gene dosage effects.

cg22443212 is located upstream of the coding area of AAA^+ ATPases and RING finger domains. RNF213 has two AAA^+ ATPase modules; the first module is essential for assembling RNF213 oligomers, whereas the second module is essential for the disassembly of RNF213 oligomers[37]. Conformational changes in modules are assumed to be related to RNF213 function[37, 47]. In addition, a considerable amount of data supported the idea that the RING finger domain possibly acts as a ubiquitin ligase that covalently modifies substrate proteins with ubiquitin and stimulates intracellular biological processes[37, 48]. Based on previous and present study results, it is reasonable to infer that the hypermethylation of cg22443212 might affect the expression of the downstream genetic information, for example, by blocking the binding of transcription factors or methyl-binding proteins, thus altering the function and/or activity of RNF213. Of course, the precise molecular mechanism by which DNA methylation of *Rnf213* causes human ICAS needs further investigation. In all, our findings, together with previously published susceptible mutation sites of *Rnf213*, suggest that there might be many more genetic or epigenetic abnormalities of *Rnf213* in ICAS, and whether these polymorphisms affect gene expression related to DNA methylation needs further studies.

There are several limitations in our study. First, intracranial arteries were assessed by MRA, CTA, or DSA. Different methods may lead to differences in severity assessments. In fact, all the patients received CTA and/or DSA. It has been demonstrated that CTA has high sensitivity and specificity for detecting ≥ 50% stenosis of large intracranial arterial segments compared to DSA[49]. Second, we measured DNA methylation levels in peripheral blood leucocytes rather than in vessels. DNA methylation patterns are largely conserved across tissues and individuals[50]. In addition, considering that harvesting intracranial arteries from a human body is impractical, the research strategy used in this study was ethical and logical. Third, due to the relatively small sample size analyzed in our study, aberrant methylation sites were not analyzed with clinical parameters, and functional analysis were not adjusted using the False discovery rate FDR-controlling procedures or the Bonferroni correction. Besides, differences in DNA collection without adjustments of cell-type composition may bring in additional systematic biases[51]. Thus, larger sample sizes are required in future studies. Nevertheless, this study constitutes the first preliminary identification of DNA methylation patterns in patients with ICAS and may help us to understand ICAS-associated genetic–epigenetic interactions.

Conclusion

In conclusion, the present study is a preliminary exploration of DNA methylation in patients with early-onset ICAS and controls. Overall, differentially methylated sites, corresponding genes, and associated biological processes and pathways were identified on the basis of the Infinium Human MethylationEPIC BeadChip interrogation and functional analysis, providing direct evidence that DNA methylation might play an important role in the occurrence and development of ICAS. In addition, we also identified and validated a significantly hypermethylated site in the gene *Rnf213* for the first time, supporting the functional relevance of methylation of *Rnf213* in ICAS. In the future, studies that further validate the differential methylation of CpG sites are needed.

Conflict of Interest

The authors declare no conflicts of interest.

Grant Support

This work was supported by the Biomedicine Key program of the Shanghai Municipal Science and Technology Commission [No. 16411953100 to J.-R. Liu], the National Natural Science Foundation of China [No. 31400838 to G.-H. Cui and No. 81271302 to J.-R. Liu], a science popularization project and research innovation project from the Shanghai Municipal Science and Technology Commission [No. 18dz2313603 and No. 14JC1404300 to J.-R. Liu],

the "Prevention and Control of Chronic Diseases Project" of Shanghai Hospital Development Center [No. SHDC12015310 to J.-R. Liu], a project from Shanghai Municipal Education Commission-Gaofeng Clinical Medicine Grant Support [No. 20161422 to J.-R. Liu], and the Clinical Research Project from Shanghai Jiao Tong University School of Medicine [No. DLY201614 to J.-R. Liu].

References

1) Gorelick PB, Wong KS, Bae HJ and Pandey DK: Large artery intracranial occlusive disease: a large worldwide burden but a relatively neglected frontier. Stroke, 2008; 39: 2396-2399
2) Pu Y, Lan L, Leng X, Wong LK and Liu L: Intracranial atherosclerosis: From anatomy to pathophysiology. Int J Stroke, 2017; 12: 236-245
3) Wang Y, Zhao X, Liu L, Soo YO, Pu Y, Pan Y, Wang Y, Zou X, Leung TW, Cai Y, Bai Q, Wu Y, Wang C, Pan X, Luo B and Wong KS: Prevalence and outcomes of symptomatic intracranial large artery stenoses and occlusions in China: the Chinese Intracranial Atherosclerosis (CICAS) Study. Stroke, 2014; 45: 663-669
4) Suzuki MM and Bird A: DNA methylation landscapes: provocative insights from epigenomics. Nat Rev Genet, 2008; 9: 465-476
5) Heyn H and Esteller M: DNA methylation profiling in the clinic: applications and challenges. Nat Rev Genet, 2012; 13: 679-692
6) Valencia-Morales Mdel P, Zaina S, Heyn H, Carmona FJ, Varol N, Sayols S, Condom E, Ramirez-Ruz J, Gomez A, Moran S, Lund G, Rodriguez-Rios D, Lopez-Gonzalez G, Ramirez-Nava M, de la Rocha C, Sanchez-Flores A and Esteller M: The DNA methylation drift of the atherosclerotic aorta increases with lesion progression. BMC Med Genomics, 2015; 8: 015-0085
7) Jiang YZ, Manduchi E, Stoeckert CJ, Jr. and Davies PF: Arterial endothelial methylome: differential DNA methylation in athero-susceptible disturbed flow regions in vivo. BMC Genomics, 2015; 16: 015-1656
8) Horvath S, Gurven M, Levine ME, Trumble BC, Kaplan H, Allayee H, Ritz BR, Chen B, Lu AT, Rickabaugh TM, Jamieson BD, Sun D, Li S, Chen W, Quintana-Murci L, Fagny M, Kobor MS, Tsao PS, Reiner AP, Edlefsen KL, Absher D and Assimes TL: An epigenetic clock analysis of race/ethnicity, sex, and coronary heart disease. Genome Biol, 2016; 17: 016-1030
9) Irvin MR, Zhi D, Joehanes R, Mendelson M, Aslibekyan S, Claas SA, Thibeault KS, Patel N, Day K, Jones LW, Liang L, Chen BH, Yao C, Tiwari HK, Ordovas JM, Levy D, Absher D and Arnett DK: Epigenome-wide association study of fasting blood lipids in the Genetics of Lipid-lowering Drugs and Diet Network study. Circulation, 2014; 130: 565-572
10) Dick KJ, Nelson CP, Tsaprouni L, Sandling JK, Aissi D, Wahl S, Meduri E, Morange PE, Gagnon F, Grallert H, Waldenberger M, Peters A, Erdmann J, Hengstenberg C, Cambien F, Goodall AH, Ouwehand WH, Schunkert H, Thompson JR, Spector TD, Gieger C, Tregouet DA, Deloukas P and Samani NJ: DNA methylation and body-mass index: a genome-wide analysis. Lancet, 2014; 383: 1990-1998
11) Hidalgo B, Irvin MR, Sha J, Zhi D, Aslibekyan S, Absher D, Tiwari HK, Kabagambe EK, Ordovas JM and Arnett DK: Epigenome-wide association study of fasting measures of glucose, insulin, and HOMA-IR in the Genetics of Lipid Lowering Drugs and Diet Network study. Diabetes, 2014; 63: 801-807
12) D'Armiento FP, Bianchi A, de Nigris F, Capuzzi DM, D'Armiento MR, Crimi G, Abete P, Palinski W, Condorelli M and Napoli C: Age-related effects on atherogenesis and scavenger enzymes of intracranial and extracranial arteries in men without classic risk factors for atherosclerosis. Stroke, 2001; 32: 2472-2479
13) Napoli C, Witztum JL, de Nigris F, Palumbo G, D'Armiento FP and Palinski W: Intracranial arteries of human fetuses are more resistant to hypercholesterolemia-induced fatty streak formation than extracranial arteries. Circulation, 1999; 99: 2003-2010
14) Zaina S, Goncalves I, Carmona FJ, Gomez A, Heyn H, Mollet IG, Moran S, Varol N and Esteller M: DNA methylation dynamics in human carotid plaques after cerebrovascular events. Arterioscler Thromb Vasc Biol, 2015; 35: 1835-1842
15) Soriano-Tarraga C, Mola-Caminal M, Giralt-Steinhauer E, Ois A, Rodriguez-Campello A, Cuadrado-Godia E, Gomez-Gonzalez A, Vivanco-Hidalgo RM, Fernandez-Cadenas I, Cullell N, Roquer J and Jimenez-Conde J: Biological age is better than chronological as predictor of 3-month outcome in ischemic stroke. Neurology, 2017; 89: 830-836
16) Horvath S and Raj K: DNA methylation-based biomarkers and the epigenetic clock theory of ageing. Nat Rev Genet, 2018; 19: 371-384
17) Xu S, Cheng J, Li NH, Chen YN, Cai MY, Tang SS, Huang H, Zhang B, Cen JM, Yang XL, Chen C, Liu X and Xiong XD: The association of APOC4 polymorphisms with premature coronary artery disease in a Chinese Han population. Lipids Health Dis, 2015; 14: 015-0065
18) Suwa M, Imoto T, Kida A, Yokochi T, Iwase M and Kozawa K: Association of body flexibility and carotid atherosclerosis in Japanese middle-aged men: a cross-sectional study. BMJ Open, 2018; 8: e019370
19) Chimowitz MI, Kokkinos J, Strong J, Brown MB, Levine SR, Silliman S, Pessin MS, Weichel E, Sila CA, Furlan AJ and et al.: The Warfarin-Aspirin Symptomatic Intracranial Disease Study. Neurology, 1995; 45: 1488-1493
20) Han W, Shi M and Spivack SD: Site-specific methylated reporter constructs for functional analysis of DNA methylation. Epigenetics, 2013; 8: 1176-1187
21) Bahar Halpern K, Vana T and Walker MD: Paradoxical role of DNA methylation in activation of FoxA2 gene expression during endoderm development. J Biol Chem, 2014; 289: 23882-23892
22) Sonobe S, Fujimura M, Niizuma K, Nishijima Y, Ito A, Shimizu H, Kikuchi A, Arai-Ichinoi N, Kure S and Tominaga T: Temporal profile of the vascular anatomy evaluated by 9.4-T magnetic resonance angiography and histo-

pathological analysis in mice lacking RNF213: a susceptibility gene for moyamoya disease. Brain Res, 2014; 13: 64-71
23) Liu W, Morito D, Takashima S, Mineharu Y, Kobayashi H, Hitomi T, Hashikata H, Matsuura N, Yamazaki S, Toyoda A, Kikuta K, Takagi Y, Harada KH, Fujiyama A, Herzig R, Krischek B, Zou L, Kim JE, Kitakaze M, Miyamoto S, Nagata K, Hashimoto N and Koizumi A: Identification of RNF213 as a susceptibility gene for moyamoya disease and its possible role in vascular development. PLoS One, 2011; 6: e22542
24) Lu X: Impact of Macrophages in Atherosclerosis. Curr Med Chem, 2016; 23: 1926-1937
25) Badimon L, Storey RF and Vilahur G: Update on lipids, inflammation and atherothrombosis. Thromb Haemost, 2011; 105: 11-0717
26) Zhao J, Forsberg CW, Goldberg J, Smith NL and Vaccarino V: MAOA promoter methylation and susceptibility to carotid atherosclerosis: role of familial factors in a monozygotic twin sample. BMC Med Genet, 2012; 13: 1471-2350
27) Guarrera S, Fiorito G, Onland-Moret NC, Russo A, Agnoli C, Allione A, Di Gaetano C, Mattiello A, Ricceri F, Chiodini P, Polidoro S, Frasca G, Verschuren MWM, Boer JMA, Iacoviello L, van der Schouw YT, Tumino R, Vineis P, Krogh V, Panico S, Sacerdote C and Matullo G: Gene-specific DNA methylation profiles and LINE-1 hypomethylation are associated with myocardial infarction risk. Clin Epigenetics, 2015; 7: 015-0164
28) Fernandez-Sanles A, Sayols-Baixeras S, Subirana I, Degano IR and Elosua R: Association between DNA methylation and coronary heart disease or other atherosclerotic events: A systematic review. Atherosclerosis, 2017; 263: 325-333
29) Istas G, Declerck K, Pudenz M, Szic KSV, Lendinez-Tortajada V, Leon-Latre M, Heyninck K, Haegeman G, Casasnovas JA, Tellez-Plaza M, Gerhauser C, Heiss C, Rodriguez-Mateos A and Berghe WV: Identification of differentially methylated BRCA1 and CRISP2 DNA regions as blood surrogate markers for cardiovascular disease. Sci Rep, 2017; 7: 017-03434
30) Kucher AN, Nazarenko MS, Markov AV, Koroleva IA and Barbarash OL: Variability of Methylation Profiles of CpG Sites in microrNA Genes in Leukocytes and Vascular Tissues of Patients with Atherosclerosis. Biochemistry, 2017; 82: 698-706
31) Lund G, Andersson L, Lauria M, Lindholm M, Fraga MF, Villar-Garea A, Ballestar E, Esteller M and Zaina S: DNA methylation polymorphisms precede any histological sign of atherosclerosis in mice lacking apolipoprotein E. J Biol Chem, 2004; 279: 29147-29154
32) Abe J and Berk BC: Novel mechanisms of endothelial mechanotransduction. Arterioscler Thromb Vasc Biol, 2014; 34: 2378-2386
33) Nigro P, Abe J, Woo CH, Satoh K, McClain C, O'Dell MR, Lee H, Lim JH, Li JD, Heo KS, Fujiwara K and Berk BC: PKCzeta decreases eNOS protein stability via inhibitory phosphorylation of ERK5. Blood, 2010; 116: 1971-1979
34) Kuang HJ, Zhao GJ, Chen WJ, Zhang M, Zeng GF, Zheng XL and Tang CK: Hsp27 promotes ABCA1 expression and cholesterol efflux through the PI3K/PKC-zeta/Sp1 pathway in THP-1 macrophages. European journal of pharmacology, 2017; 810: 57-62
35) Xu L, Zheng D, Wang L, Jiang D, Liu H, Xu L, Liao Q, Zhang L, Liu P, Shi X, Wang Z, Sun L, Zhou Q, Li N, Huang Y, Le Y, Ye M, Shao G and Duan S: GCK gene-body hypomethylation is associated with the risk of coronary heart disease. Biomed Res Int, 2014: 151723
36) Garcia-Cardona MC, Huang F, Garcia-Vivas JM, Lopez-Camarillo C, Del Rio Navarro BE, Navarro Olivos E, Hong-Chong E, Bolanos-Jimenez F and Marchat LA: DNA methylation of leptin and adiponectin promoters in children is reduced by the combined presence of obesity and insulin resistance. International journal of obesity (2005), 2014; 38: 1457-1465
37) Morito D, Nishikawa K, Hoseki J, Kitamura A, Kotani Y, Kiso K, Kinjo M, Fujiyoshi Y and Nagata K: Moyamoya disease-associated protein mysterin/RNF213 is a novel AAA+ ATPase, which dynamically changes its oligomeric state. Sci Rep, 2014; 4:4442
38) Scholz B, Korn C, Wojtarowicz J, Mogler C, Augustin I, Boutros M, Niehrs C and Augustin HG: Endothelial RSPO3 Controls Vascular Stability and Pruning through Non-canonical WNT/Ca(2+)/NFAT Signaling. Dev Cell, 2016; 36: 79-93
39) Ohkubo K, Sakai Y, Inoue H, Akamine S, Ishizaki Y, Matsushita Y, Sanefuji M, Torisu H, Ihara K, Sardiello M and Hara T: Moyamoya disease susceptibility gene RNF213 links inflammatory and angiogenic signals in endothelial cells. Sci Rep, 2015; 5:13191
40) Kanoke A, Fujimura M, Niizuma K, Fujimura T, Kakizaki A, Ito A, Sakata H, Sato-Maeda M, Kure S and Tominaga T: Temporal profile of magnetic resonance angiography and decreased ratio of regulatory T cells after immunological adjuvant administration to mice lacking RNF213, a susceptibility gene for moyamoya disease. Brain Res, 2016; 1: 1-9
41) Duan L, Wei L, Tian Y, Zhang Z, Hu P, Wei Q, Liu S, Zhang J, Wang Y, Li D, Yang W, Zong R, Xian P, Han C, Bao X, Zhao F, Feng J, Liu W, Cao W, Zhou G, Zhu C, Yu F, Yang W, Meng Y, Wang J, Chen X, Wang Y, Shen B, Zhao B, Wan J, Zhang F, Zhao G, Xu A, Zhang X, Liu J, Zuo X and Wang K: Novel Susceptibility Loci for Moyamoya Disease Revealed by a Genome-Wide Association Study. Stroke, 2018; 49: 11-18
42) Miyawaki S, Imai H, Takayanagi S, Mukasa A, Nakatomi H and Saito N: Identification of a genetic variant common to moyamoya disease and intracranial major artery stenosis/occlusion. Stroke, 2012; 43: 3371-3374
43) Miyawaki S, Imai H, Shimizu M, Yagi S, Ono H, Mukasa A, Nakatomi H, Shimizu T and Saito N: Genetic variant RNF213 c.14576G>A in various phenotypes of intracranial major artery stenosis/occlusion. Stroke, 2013; 44: 2894-2897
44) Bang OY, Chung JW, Cha J, Lee MJ, Yeon JY, Ki CS, Jeon P, Kim JS and Hong SC: A Polymorphism in RNF213 Is a Susceptibility Gene for Intracranial Atherosclerosis. PLoS One, 2016; 11: e0156607
45) Zhou S, Ambalavanan A, Rochefort D, Xie P, Bourassa CV, Hince P, Dionne-Laporte A, Spiegelman D, Gan-Or Z, Mirarchi C, Zaharieva V, Dupre N, Kobayashi H,

Hitomi T, Harada K, Koizumi A, Xiong L, Dion PA and Rouleau GA: RNF213 Is Associated with Intracranial Aneurysms in the French-Canadian Population. Am J Hum Genet, 2016; 99: 1072-1085
46) Miyatake S, Miyake N, Touho H, Nishimura-Tadaki A, Kondo Y, Okada I, Tsurusaki Y, Doi H, Sakai H, Saitsu H, Shimojima K, Yamamoto T, Higurashi M, Kawahara N, Kawauchi H, Nagasaka K, Okamoto N, Mori T, Koyano S, Kuroiwa Y, Taguri M, Morita S, Matsubara Y, Kure S and Matsumoto N: Homozygous c.14576G>A variant of RNF213 predicts early-onset and severe form of moyamoya disease. Neurology, 2012; 78: 803-810
47) Kobayashi H, Matsuda Y, Hitomi T, Okuda H, Shioi H, Matsuda T, Imai H, Sone M, Taura D, Harada KH, Habu T, Takagi Y, Miyamoto S and Koizumi A: Biochemical and Functional Characterization of RNF213 (Mysterin) R4810K, a Susceptibility Mutation of Moyamoya Disease, in Angiogenesis In Vitro and In Vivo. J Am Heart Assoc, 2015; 4: 002146
48) Deshaies RJ and Joazeiro CA: RING domain E3 ubiquitin ligases. Annu Rev Biochem, 2009; 78: 399-434
49) Nguyen-Huynh MN, Wintermark M, English J, Lam J, Vittinghoff E, Smith WS and Johnston SC: How accurate is CT angiography in evaluating intracranial atherosclerotic disease? Stroke, 2008; 39: 1184-1188
50) Byun HM, Siegmund KD, Pan F, Weisenberger DJ, Kanel G, Laird PW and Yang AS: Epigenetic profiling of somatic tissues from human autopsy specimens identifies tissue- and individual-specific DNA methylation patterns. Hum Mol Genet, 2009; 18: 4808-4817
51) Shiwa Y, Hachiya T, Furukawa R, Ohmomo H, Ono K, Kudo H, Hata J, Hozawa A, Iwasaki M, Matsuda K, Minegishi N, Satoh M, Tanno K, Yamaji T, Wakai K, Hitomi J, Kiyohara Y, Kubo M, Tanaka H, Tsugane S, Yamamoto M, Sobue K and Shimizu A: Adjustment of Cell-Type Composition Minimizes Systematic Bias in Blood DNA Methylation Profiles Derived by DNA Collection Protocols. PLoS One, 2016; 11: e0147519

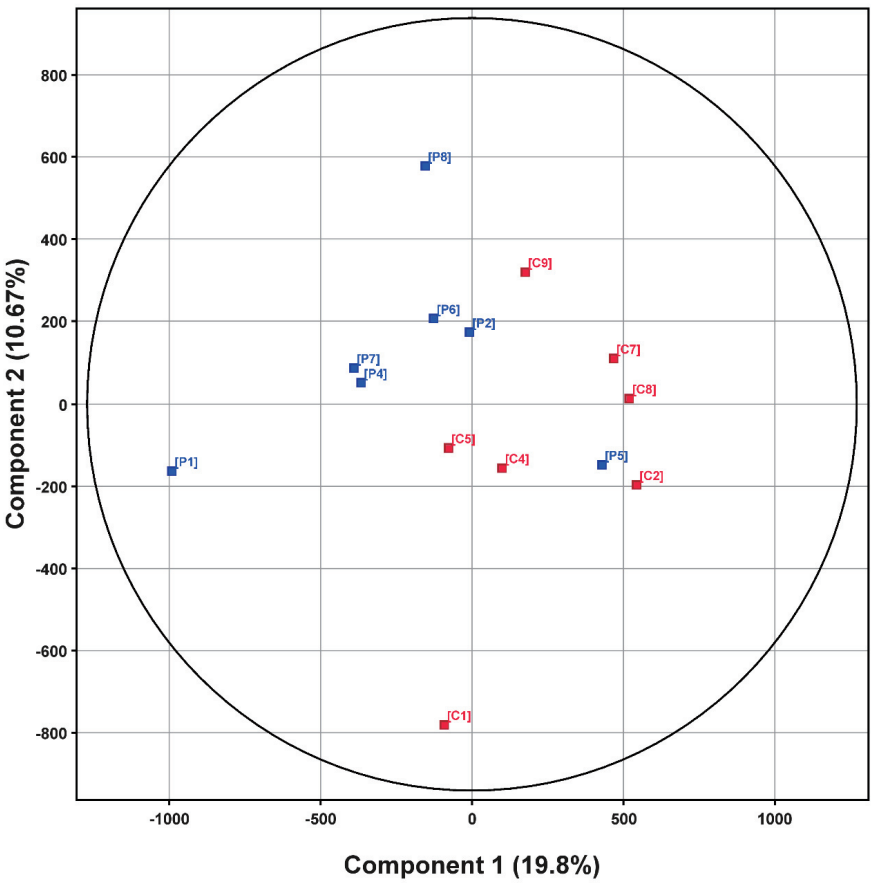

Supplementary Fig. 1. Principal component analysis (PCA) for the DNA methylation levels of the samples

PCA was performed using the full microarray data from patients (blue points) and controls (red points) and showed two independent clusters.

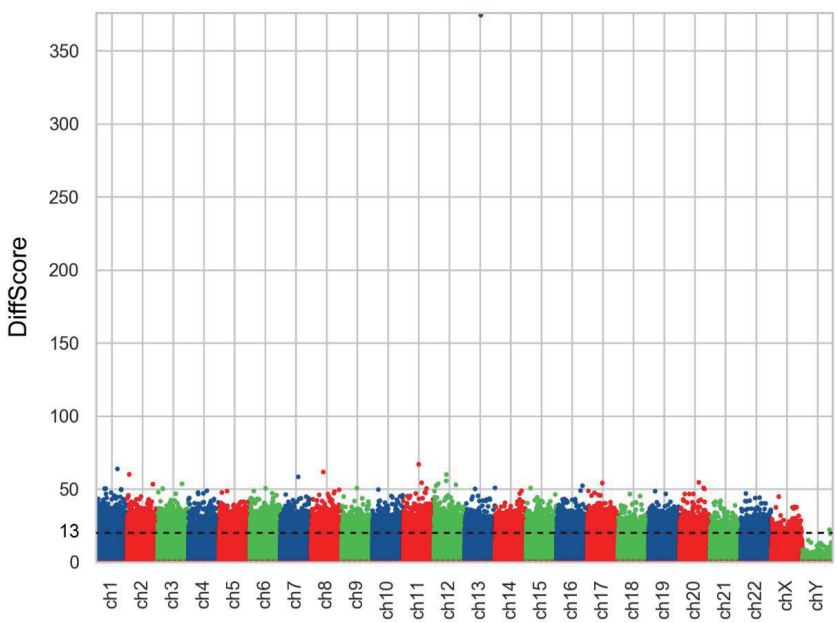

Supplementary Fig. 2. Manhattan plots showing distribution of possible differentially methylated CpG sites identified in this study across chromosomes

The black dotted horizontal line indicates the genome-wide significance threshold of an absolute value of DiffScore >13.

Supplementary Table 1. Baseline and clinical characteristics of the participants for pyrosequencing

Characteristic	Patients (n = 21)	Controls (n = 21)	P value
Demographics			
Age (years)	55 (48, 59)	57 (53, 59)	0.732
Male (%)	19 (90.5)	19 (90.5)	1.000
Hypertension (%)	17 (81.0)	12 (57.1)	0.181
Diabetes mellitus (%)	8 (38.1)	8 (38.1)	1.000
Dyslipidaemia (%)	14 (66.7)	10 (47.6)	0.350
Smoking (%)	15 (71.4)	14 (66.7)	1.000
Drinking (%)	8 (38.1)	8 (38.1)	1.000
SBP (mmHg)	148.1 ± 19.6	144.0 ± 28.0	0.585
DBP (mmHg)	80.8 ± 10.0	86.9 ± 28.0	0.164
Laboratory parameters			
FBG (mmol/L)	5.85 (5.05, 6.95)	5.85 (5.53, 6.35)	0.886
TG (mmol/L)	1.85 (1.22, 2.09)	1.73 (1.12, 2.48)	0.940
TC (mmol/L)	3.85 (3.45, 4.87)	3.80 (3.41, 4.08)	0.725
HDL-C (mmol/L)	0.87 ± 0.19	0.91 ± 0.25	0.550
LDL-C (mmol/L)	2.79 ± 1.00	2.58 ± 0.98	0.504
Homocysteine (μmol/L)	15.60 (11.20, 27.30)	13.00 (10.93, 17.38)	0.210
Fibrinogen (g/L)	2.47 (2.04, 2.97)	2.37 (2.07, 2.60)	0.355
CRP (mg/L)	3.39 (3.09, 6.50)	3.30 (3.02, 3.74)	0.402
Urea nitrogen (mmol/L)	5.00 (4.18, 6.48)	5.00 (3.88, 6.25)	0.507
Uric acid (μmol/L)	282.67 ± 78.60	316.68 ± 77.62	0.177
Creatinine (μmol/L)	85.00 (74.50, 96.75)	86.50 (78.00, 96.25)	0.979

Continuous variables are expressed as the mean ± standard deviation or the median (interquartile range). Categorical values are presented as frequencies (percentages).
Abbreviations: SBP, systolic blood pressure; DBP, diastolic blood pressure; FBG, fasting blood glucose; TG, triglycerides; TC, total cholesterol; HDL-C, high-density lipoprotein cholesterol; LDL-C, low-density lipoprotein cholesterol; CRP, C-reactive protein.

Supplementary Table 2. Differentially methylated CpG sites between patients and controls. Single CpG with an absolute value of Diffscore >13 and an absolute value of Delta_Beta >0.17 were considered as differentially methylated loci

Serial number	CpG site ID	Chromosome	Position	UCSC_RefGene_Name	AVG_Beta in patients	AVG_Beta in controls	Delta Beta	DiffScore
1	cg08977311	3	168308798	C3orf50	0.293	0.790	-0.497	-22.578
2	cg26263138	X	47633928		0.172	0.650	-0.478	-23.065
3	cg17348244	7	786861	HEATR2	0.173	0.630	-0.457	-15.396
4	cg16661266	13	31819391	B3GLCT	0.307	0.759	-0.452	-14.175
5	cg08522473	3	111730545	TAGLN3; TAGLN3; TAGLN3	0.287	0.727	-0.440	-18.498
6	cg03749159	8	133714769		0.361	0.793	-0.433	-18.496
7	cg10123377	3	42387524		0.312	0.717	-0.405	-22.520
8	cg13239126	1	15256136	KIAA1026; KIAA1026; KIAA1026; KIAA1026	0.359	0.757	-0.397	-18.024
9	cg21838924	7	73245103	CLDN4	0.405	0.801	-0.396	-18.998
10	cg10930703	18	43570033	PSTPIP2	0.452	0.840	-0.388	-17.581
11	cg24398793	7	15651770	MEOX2	0.227	0.613	-0.386	-17.868
12	cg21741515	3	196048411		0.269	0.651	-0.383	-14.615
13	cg21714731	3	79701155	ROBO1	0.215	0.597	-0.381	-19.551
14	cg02866897	20	37470452	PPP1R16B; PPP1R16B	0.210	0.582	-0.372	-15.444
15	cg03136151	1	92415048	BRDT; BRDT	0.465	0.835	-0.369	-18.434
16	cg16037139	6	47040730		0.465	0.833	-0.368	-16.434
17	cg00814186	17	74585455		0.254	0.616	-0.363	-17.294
18	cg04307318	6	56244487	RNU6-71P	0.217	0.577	-0.360	-13.060
19	cg26588921	1	40183922		0.227	0.587	-0.360	-23.434
20	cg05192017	12	115273077		0.085	0.439	-0.354	-25.129
21	cg10765459	21	47524956	COL6A2; COL6A2; COL6A2	0.391	0.744	-0.353	-14.405
22	cg03221390	1	247803637		0.091	0.440	-0.349	-23.252
23	cg16310958	20	25281332	ABHD12; ABHD12	0.089	0.433	-0.344	-13.666
24	cg21415084	12	84218134		0.400	0.741	-0.341	-16.413
25	cg21130926	20	46415320	SULF2; SULF2; SULF2; SULF2; SULF2	0.485	0.820	-0.335	-15.902
26	cg13920856	2	159867184	TANC1; TANC1	0.352	0.680	-0.327	-16.415
27	cg15441831	7	73245178	CLDN4	0.447	0.772	-0.325	-17.383
28	cg11282840	8	49057154		0.486	0.810	-0.324	-35.283
29	cg18444757	18	12035841		0.085	0.408	-0.323	-13.591
30	cg01359658	7	2426868		0.421	0.743	-0.322	-13.715
32	cg11016221	9	132505647	PTGES	0.472	0.783	-0.311	-24.572
33	cg07227024	2	202163482	ALS2CR12; ALS2CR12	0.221	0.529	-0.308	-19.581
34	cg24329141	10	27095369	ABI1; ABI1; ABI1; ABI1	0.608	0.915	-0.307	-40.978
35	cg00740510	22	43811071	MPPED1	0.184	0.489	-0.306	-14.400
36	cg06995503	10	3178915	PFKP	0.585	0.888	-0.302	-27.762
37	cg02794920	3	23243300	UBE2E2	0.498	0.797	-0.298	-13.903
38	cg16935517	10	11577115	USP6NL	0.446	0.738	-0.292	-15.934
39	cg04998153	1	101823331	LINC01307	0.310	0.600	-0.290	-19.385
40	cg22786333	7	801211	HEATR2	0.358	0.643	-0.285	-15.330
41	cg07469467	12	99092857	APAF1; APAF1; APAF1; APAF1; APAF1	0.077	0.360	-0.284	-22.648
42	cg07895205	1	94240679	BCAR3	0.431	0.715	-0.283	-18.465
43	cg11173636	10	65632259		0.051	0.333	-0.283	-17.786
44	cg02730303	11	103480630		0.032	0.311	-0.279	-26.937
45	cg03639185	4	144207789		0.021	0.293	-0.272	-18.310
46	cg00570635	2	65355269	RAB1A; RAB1A	0.093	0.363	-0.270	-23.122
47	cg12052601	2	100900379	LONRF2	0.253	0.522	-0.268	-13.884
48	cg27281836	11	49229833	FOLH1; FOLH1	0.065	0.332	-0.267	-13.357
49	cg24022528	7	140393175	ADCK2	0.629	0.894	-0.266	-25.146

(Cont. Supplementary Table 2)

Serial number	CpG site ID	Chromosome	Position	UCSC_RefGene_Name	AVG_Beta in patients	AVG_Beta in controls	Delta Beta	DiffScore
50	cg08238375	5	112483149	MCC; MCC	0.334	0.597	-0.263	-13.575
51	cg19288863	6	133749548	EYA4; EYA4; EYA4; EYA4; EYA4	0.606	0.869	-0.263	-13.607
52	cg25249362	10	3163518	PFKP	0.644	0.902	-0.258	-17.129
53	cg05182217	7	138803256		0.381	0.637	-0.256	-16.720
54	cg00173776	1	31465032	PUM1; PUM1	0.569	0.822	-0.253	-17.894
55	cg25771369	14	20528494	OR4L1	0.355	0.607	-0.252	-17.825
56	cg16145187	17	53684393		0.466	0.713	-0.247	-17.811
57	cg00113675	6	29855347	HLA-H	0.221	0.467	-0.246	-14.165
58	cg26889118	15	49342629		0.394	0.640	-0.246	-13.043
59	cg10993865	13	111293846	CARS2	0.659	0.898	-0.239	-17.714
60	cg09258259	19	3143043	LOC100996351; GNA15; LOC100996351	0.086	0.325	-0.239	-24.665
61	cg01354003	8	6422103	ANGPT2; ANGPT2; ANGPT2; MCPH1	0.130	0.368	-0.238	-18.462
62	cg12589297	15	67136155		0.292	0.529	-0.238	-17.323
63	cg23329272	5	180085924		0.171	0.407	-0.236	-26.200
64	cg10288111	7	112062682	IFRD1	0.324	0.556	-0.232	-18.503
65	cg21932934	11	120039306		0.553	0.785	-0.232	-20.501
66	cg07138269	8	72765107	MSC-AS1; MSC-AS1	0.597	0.828	-0.231	-14.165
67	cg07056794	9	139318309		0.616	0.847	-0.231	-16.710
68	cg16033700	4	14868419	LINC00504	0.558	0.789	-0.231	-16.236
69	cg25576961	15	99709980	TTC23; TTC23; TTC23; TTC23; TTC23; TTC23; TTC23	0.538	0.769	-0.231	-13.767
70	cg05407981	2	202289316	TRAK2	0.523	0.749	-0.225	-13.664
71	cg12063064	3	48712367	NCKIPSD; NCKIPSD	0.656	0.881	-0.225	-16.775
72	cg07044859	10	101282883		0.165	0.390	-0.225	-13.591
73	cg09281805	7	4751840	FOXK1	0.639	0.863	-0.224	-19.263
74	cg18352080	1	2004953	PRKCZ; PRKCZ; PRKCZ	0.645	0.868	-0.223	-17.388
75	cg24795173	10	108751940	SORCS1; SORCS1; SORCS1; SORCS1; SORCS1; SORCS1	0.353	0.575	-0.223	-20.450
76	cg23230564	5	31470890	RNASEN; RNASEN	0.282	0.503	-0.221	-17.710
77	cg18805164	19	36265700	SNX26	0.691	0.909	-0.218	-15.024
78	cg03964373	1	241800323	CHML; OPN3	0.659	0.877	-0.218	-23.684
79	cg02631626	13	27546802		0.384	0.600	-0.216	-17.758
80	cg04610742	1	230513809	PGBD5	0.474	0.688	-0.214	-15.276
81	cg06075754	10	104169733	PSD	0.455	0.668	-0.213	-13.315
82	cg02953125	2	1079100	SNTG2	0.632	0.845	-0.213	-16.972
83	cg03971505	12	22063949	ABCC9; ABCC9	0.164	0.373	-0.209	-21.683
84	cg05990366	12	124773693	FAM101A	0.657	0.866	-0.209	-17.168
85	cg13110951	1	246746101	CNST; CNST	0.372	0.579	-0.208	-16.599
86	cg16749629	12	66459807		0.370	0.577	-0.207	-23.075
87	cg14144366	10	61764026		0.562	0.766	-0.204	-14.448
88	cg14773207	18	43567084	PSTPIP2	0.542	0.743	-0.201	-16.466
89	cg02662417	6	157161545	ARID1B; ARID1B; ARID1B	0.555	0.753	-0.198	-27.851
90	cg17888390	10	101282816		0.135	0.333	-0.198	-14.137
91	cg11233593	4	83955464	COPS4; COPS4	0.124	0.319	-0.195	-27.901
92	cg13363575	2	131967322		0.389	0.584	-0.195	-15.852
93	cg18399194	10	101918448	ERLIN1; ERLIN1	0.682	0.875	-0.193	-20.530
94	cg09235562	19	384251		0.500	0.691	-0.192	-29.468
95	cg13462557	1	62499140	INADL	0.661	0.851	-0.190	-14.527
96	cg12460140	12	77771462		0.421	0.611	-0.190	-13.579

(Cont. Supplementary Table 2)

Serial number	CpG site ID	Chromosome	Position	UCSC_RefGene_Name	AVG_Beta in patients	AVG_Beta in controls	Delta Beta	DiffScore
97	cg17789193	19	14533491		0.199	0.387	-0.189	-25.666
98	cg03185552	17	81060259		0.522	0.711	-0.189	-14.037
99	cg07590402	10	104840433		0.636	0.824	-0.188	-16.039
100	cg23221052	5	179740743	GFPT2	0.438	0.626	-0.188	-15.892
101	cg26930243	3	117482571		0.311	0.499	-0.188	-16.534
102	cg24391912	15	100259320		0.124	0.312	-0.188	-14.732
103	cg12824232	1	101842425	LINC01307	0.706	0.891	-0.185	-15.229
104	cg17113546	12	10451780		0.680	0.865	-0.185	-16.559
105	cg10001720	1	31231363	LAPTM5	0.449	0.634	-0.185	-18.501
106	cg06074563	X	107980779	LOC101928358; IRS4	0.198	0.382	-0.185	-15.015
107	cg23540632	18	67253448	DOK6	0.482	0.666	-0.184	-25.384
108	cg05850769	14	88470085	GPR65	0.284	0.468	-0.184	-15.075
109	cg00366603	6	32186049	NOTCH4	0.650	0.834	-0.184	-14.923
110	cg22188184	6	101168404	ASCC3; ASCC3	0.202	0.386	-0.183	-18.138
111	cg16706502	14	31927974	C14orf126	0.328	0.511	-0.183	-14.920
112	cg03853124	6	33875958		0.229	0.412	-0.183	-40.741
113	cg00495303	18	3771110	DLGAP1; DLGAP1	0.393	0.575	-0.182	-13.231
114	cg21743623	3	130682976	ATP2C1; ATP2C1; ATP2C1; ATP2C1	0.284	0.465	-0.181	-14.772
115	cg19707454	7	6616677	ZDHHC4; ZDHHC4; ZDHHC4; ZDHHC4	0.538	0.718	-0.180	-14.951
116	cg04345661	20	32721338		0.382	0.562	-0.180	-23.844
117	cg10356706	6	167639159		0.238	0.417	-0.179	-15.332
118	cg01501399	13	27557211		0.277	0.456	-0.179	-25.786
119	cg06304546	20	32448765		0.550	0.728	-0.178	-18.794
120	cg16201634	1	9146357		0.446	0.623	-0.178	-27.955
121	cg19224645	1	39282003		0.123	0.300	-0.177	-24.401
122	cg06715136	7	158046025	PTPRN2; PTPRN2; PTPRN2	0.686	0.862	-0.176	-16.955
123	cg17764313	3	127335263	MCM2; MCM2	0.612	0.787	-0.175	-15.379
124	cg14087524	1	38349487	INPP5B; INPP5B	0.431	0.605	-0.174	-14.982
125	cg08584759	10	11912126	C10orf47	0.654	0.828	-0.174	-15.768
126	cg06835411	4	186301987		0.630	0.803	-0.174	-14.912
127	cg00553601	1	224268136		0.642	0.815	-0.174	-13.757
128	cg20916362	3	39821326		0.625	0.798	-0.173	-15.895
129	cg26749518	19	51506165	KLK9; KLK8; KLK8; KLK8; KLK8	0.376	0.549	-0.173	-18.916
130	cg01438711	17	69789307		0.081	0.253	-0.172	-15.951
131	cg20720056	10	101910498	ERLIN1; ERLIN1	0.727	0.899	-0.172	-19.068
132	cg06637768	6	2886816	LOC101927730	0.079	0.250	-0.172	-16.451
133	cg14361804	9	117694183	TNFSF8	0.354	0.525	-0.172	-13.152
134	cg19935450	10	6281135		0.488	0.659	-0.171	-21.693
135	cg13837146	9	111548749		0.373	0.543	-0.170	-19.836
136	cg01429604	12	95264769		0.733	0.563	0.170	14.178
137	cg23100626	2	96804247	ASTL	0.699	0.527	0.171	16.154
138	cg24578857	17	17110207	PLD6	0.724	0.552	0.171	45.426
139	cg13799572	11	126382235	KIRREL3; KIRREL3; KIRREL3	0.850	0.678	0.173	13.887
140	cg12790145	12	312737	LOC101929384; SLC6A12; SLC6A12; SLC6A12; SLC6A12	0.586	0.412	0.174	15.535
141	cg21862353	2	1801628	MYT1L	0.730	0.556	0.174	15.696
142	cg14112997	22	17591088	IL17RA	0.559	0.384	0.175	-18.176
143	cg14651079	10	88428177	LDB3; LDB3; LDB3; LDB3; LDB3; LDB3	0.839	0.664	0.175	17.571

(Cont. Supplementary Table 2)

Serial number	CpG site ID	Chromosome	Position	UCSC_RefGene_Name	AVG_Beta in patients	AVG_Beta in controls	Delta Beta	DiffScore
144	cg02295574	5	1054262	SLC12A7	0.863	0.686	0.176	14.505
145	cg26337497	3	31935279	OSBPL10	0.524	0.347	0.177	15.288
146	cg16222062	14	105509229		0.948	0.770	0.178	32.118
147	cg07743747	3	46394550	CCR2; CCR2	0.514	0.336	0.178	14.127
148	cg05635359	8	39272909		0.548	0.370	0.178	21.267
149	cg00950476	12	11708930	LINC01252	0.497	0.319	0.179	17.296
150	cg19537558	5	167550996	ODZ2	0.848	0.669	0.180	14.696
151	cg11890239	8	103541014		0.512	0.333	0.180	19.714
152	cg08713344	10	3183772	PITRM1-AS1; PITRM1; PITRM1; PITRM1	0.794	0.613	0.181	19.593
153	cg11403739	15	22923741	CYFIP1	0.563	0.382	0.181	13.247
154	cg24496423	X	153046480	SRPK3; SRPK3; SRPK3; SRPK3; SRPK3; SRPK3	0.503	0.322	0.181	20.845
155	cg06001976	X	3790470		0.721	0.540	0.181	17.999
156	cg20360416	4	7246127	SORCS2	0.869	0.688	0.181	15.131
157	cg05531409	3	131637172	CPNE4	0.802	0.620	0.181	15.419
158	cg27266060	8	22091797		0.608	0.427	0.181	15.051
159	cg00525277	6	32064239	TNXB	0.653	0.470	0.184	35.837
160	cg16655091	13	26590097	ATP8A2	0.853	0.667	0.185	18.585
161	cg20964965	10	134564563	INPP5A	0.888	0.703	0.186	13.066
162	cg16645815	10	134556992	INPP5A	0.924	0.738	0.186	13.850
163	cg07639376	16	1584516	IFT140; TMEM204	0.564	0.378	0.186	13.393
164	cg10890302	6	32064246	TNXB	0.442	0.255	0.187	27.733
165	cg07524919	6	32063901	TNXB	0.660	0.472	0.188	24.523
166	cg19106932	17	61926700		0.418	0.230	0.188	18.804
167	cg15265085	6	32064588	TNXB	0.459	0.271	0.189	16.969
168	cg27625131	13	113105794		0.781	0.593	0.189	23.813
169	cg14096311	4	152117184	SH3D19; SH3D19; SH3D19	0.457	0.267	0.190	13.469
170	cg09087222	8	11720363	CTSB; CTSB; CTSB; CTSB; CTSB	0.588	0.398	0.190	29.006
171	cg26094651	2	1802045	MYT1L	0.762	0.572	0.190	13.569
172	cg10510935	1	4059661		0.498	0.307	0.191	14.195
173	cg15196197	6	32064573	TNXB	0.300	0.107	0.192	19.530
174	cg25218220	13	46895635		0.583	0.391	0.192	32.598
175	cg06892295	10	84158395	NRG3; NRG3; NRG3	0.837	0.644	0.193	13.130
176	cg00079566	3	177194742	LINC00578	0.848	0.651	0.198	14.518
177	cg27387193	6	32064032	TNXB	0.598	0.400	0.198	35.411
178	cg17253931	8	127448577		0.887	0.688	0.200	19.229
179	cg22443212	17	78253912	RNF213; RNF213	0.719	0.518	0.201	18.659
180	cg06120313	11	3174092	OSBPL5; OSBPL5; OSBPL5	0.650	0.448	0.202	21.043
181	cg17608381	6	29911550	HLA-A	0.683	0.480	0.203	21.019
182	cg13914841	16	75303457		0.739	0.536	0.203	14.813
183	cg10025714	1	149150959		0.629	0.425	0.204	18.853
184	cg08880082	14	90165664		0.863	0.658	0.205	14.631
185	cg23688827	1	18767776		0.843	0.637	0.205	15.325
186	cg12038518	11	128105129		0.794	0.588	0.206	15.038
187	cg25533133	13	113664019	MCF2L; MCF2L	0.628	0.421	0.207	25.440
188	cg05460746	8	103541045		0.362	0.155	0.207	32.908
189	cg16834823	6	32064218	TNXB	0.447	0.239	0.208	38.064
190	cg13400512	6	32064578	TNXB	0.382	0.173	0.209	21.644
191	cg04175473	10	134563870	INPP5A	0.901	0.691	0.210	15.328

(Cont. Supplementary Table 2)

Serial number	CpG site ID	Chromosome	Position	UCSC_RefGene_Name	AVG_Beta in patients	AVG_Beta in controls	Delta Beta	DiffScore
192	cg04608779	6	54878849		0.765	0.555	0.210	16.652
193	cg09035930	12	129282057	SLC15A4	0.781	0.568	0.212	13.274
194	cg12432807	17	39094308	KRT23	0.898	0.684	0.214	19.471
195	cg01412970	17	17109239	PLD6	0.407	0.193	0.215	17.029
196	cg12694372	6	32064582	TNXB	0.430	0.213	0.217	19.309
197	cg11424828	8	2075469	MYOM2	0.234	0.017	0.217	13.337
198	cg01397495	2	136496804		0.724	0.507	0.217	16.881
199	cg12424998	1	174959080	RABGAP1L; RABGAP1L	0.810	0.592	0.218	14.747
200	cg05093818	4	87282697	MAPK10; MAPK10; MAPK10	0.818	0.598	0.220	19.092
201	cg22067481	19	53234126	ZNF611; ZNF611; ZNF611; ZNF611	0.887	0.666	0.221	18.721
202	cg00191853	8	101177733	SPAG1; SPAG1	0.698	0.476	0.222	13.329
203	cg25637655	6	29911542	HLA-A	0.438	0.215	0.223	17.393
204	cg07792871	6	29942706	HCG9	0.550	0.326	0.224	13.528
205	cg13671412	19	5335254	PTPRS; PTPRS; PTPRS; PTPRS	0.883	0.659	0.224	13.795
206	cg12973586	2	136553925	LCT	0.798	0.573	0.224	15.998
207	cg01992382	6	32064212	TNXB	0.462	0.237	0.225	38.432
208	cg14016372	2	86184239		0.889	0.663	0.226	18.108
209	cg10923662	6	32064258	TNXB	0.431	0.206	0.226	23.787
210	cg27395310	18	58996785		0.774	0.545	0.229	14.643
211	cg09768654	X	153046386	SRPK3; SRPK3; SRPK3	0.569	0.340	0.229	29.020
212	cg11047442	8	142852219		0.858	0.629	0.230	15.610
213	cg03979311	5	54319996	GZMK	0.636	0.406	0.230	15.043
214	cg04316537	2	102589889		0.732	0.500	0.231	23.181
215	cg25303761	1	31256028		0.422	0.189	0.233	16.501
216	cg17248267	2	36815511	FEZ2; FEZ2	0.709	0.474	0.235	13.269
217	cg12386614	1	33608053		0.881	0.645	0.236	18.948
218	cg10818676	1	167098094	DUSP27	0.271	0.034	0.236	18.208
219	cg24417798	12	124791649	FAM101A	0.906	0.663	0.242	15.896
220	cg12230162	X	153046482	SRPK3; SRPK3; SRPK3; SRPK3; SRPK3; SRPK3	0.559	0.317	0.242	23.744
221	cg14188106	6	32063895	TNXB	0.619	0.375	0.244	25.495
222	cg04467639	11	14495049	COPB1; COPB1; COPB1	0.732	0.485	0.248	15.197
223	cg16797344	18	44333132	ST8SIA5; ST8SIA5; ST8SIA5	0.762	0.515	0.248	13.546
225	cg04481635	6	224813		0.819	0.570	0.249	15.246
226	cg24686902	17	6558231		0.810	0.560	0.250	17.754
227	cg14942092	10	133787629	BNIP3	0.619	0.368	0.251	13.183
228	cg23944405	11	30602030	MPPED2; MPPED2; MPPED2	0.890	0.639	0.251	16.143
229	cg09232555	8	11619866		0.751	0.497	0.254	15.327
230	cg07484246	3	132386149	UBA5; NPHP3-ACAD11; UBA5	0.891	0.633	0.257	15.908
231	cg05058762	12	52667743		0.722	0.464	0.259	13.993
232	cg27557782	3	127256188		0.764	0.504	0.260	13.585
233	cg24638356	3	14755220	C3orf20	0.679	0.417	0.262	16.304
234	cg08750459	17	6558815		0.641	0.378	0.263	18.777
235	cg16529483	X	153046451	SRPK3; SRPK3; SRPK3	0.555	0.291	0.264	18.061
236	cg24844518	5	156811669	CYFIP2; CYFIP2; CYFIP2	0.313	0.048	0.265	17.813
237	cg11786587	5	178208610		0.882	0.615	0.267	20.983
238	cg01299494	1	161698811		0.586	0.317	0.269	13.159
239	cg01201054	12	79197569		0.874	0.604	0.270	16.871
240	cg11946459	6	29911558	HLA-A	0.696	0.424	0.272	23.466
241	cg20070588	7	66440232		0.616	0.339	0.277	16.836

(Cont. Supplementary Table 2)

Serial number	CpG site ID	Chromosome	Position	UCSC_RefGene_Name	AVG_Beta in patients	AVG_Beta in controls	Delta Beta	DiffScore
242	cg20722168	4	38832495	TLR6	0.831	0.553	0.279	13.068
243	cg08238516	17	44820121	NSF; NSF	0.394	0.113	0.281	14.005
244	cg27160885	15	74014211		0.763	0.481	0.282	15.587
245	cg03812172	7	44184403	GCK; GCK; GCK	0.767	0.484	0.283	16.714
246	cg15930509	7	128078177		0.837	0.554	0.283	13.256
247	cg01995986	6	147289366	STXBP5-AS1	0.679	0.393	0.286	15.948
248	cg06653848	11	109566635		0.677	0.390	0.287	14.604
249	cg06443038	9	35904531		0.735	0.448	0.287	21.037
250	cg23168520	13	114775133	RASA3	0.788	0.501	0.287	15.942
251	cg21358336	17	6558440		0.800	0.510	0.290	18.983
252	cg07935157	6	101403850		0.746	0.456	0.290	14.625
253	cg18232235	12	11700321		0.980	0.687	0.293	18.573
254	cg04627621	17	61970171		0.667	0.371	0.295	15.388
255	cg01710670	16	15018856		0.609	0.313	0.296	17.487
256	cg11190351	14	37458914	SLC25A21; SLC25A21	0.816	0.520	0.296	20.493
257	cg16044734	17	41824694		0.813	0.516	0.297	19.942
258	cg21878369	19	53194695	ZNF83	0.417	0.117	0.299	27.587
259	cg15290312	17	76897139	TIMP2	0.972	0.669	0.303	17.303
260	cg05861138	14	77376872		0.848	0.544	0.304	14.207
261	cg09022647	8	39328883	ADAM3A; ADAM3A; ADAM3A; ADAM3A	0.768	0.461	0.308	17.477
262	cg23390607	11	74118907		0.759	0.451	0.308	18.736
263	cg19651115	12	11700343		0.766	0.455	0.312	18.107
264	cg13885829	1	17482041		0.770	0.458	0.312	15.470
265	cg04918505	X	69716726	DLG3; DLG3; DLG3	0.719	0.407	0.312	14.250
266	cg23019589	5	10091925		0.728	0.415	0.313	15.077
267	cg06615479	17	9728771	GLP2R	0.803	0.488	0.315	22.675
268	cg10051493	16	1939295		0.902	0.584	0.318	17.531
269	cg13081429	1	236175585	NID1	0.899	0.578	0.322	13.480
270	cg09222892	1	25734099	RHCE; RHCE; RHCE; RHCE	0.698	0.375	0.323	17.287
271	cg00546757	5	170845058		0.707	0.380	0.327	13.545
272	cg26450240	11	49003361		0.739	0.412	0.328	14.257
273	cg16858433	2	45383756		0.892	0.563	0.329	13.031
274	cg18105134	13	113819100	PROZ	0.770	0.436	0.334	21.173
275	cg13805962	5	159391842	ADRA1B	0.905	0.570	0.335	19.461
276	cg25259265	13	114100875	ADPRHL1; ADPRHL1	0.778	0.442	0.336	15.913
277	cg15211026	2	65639543	SPRED2	0.846	0.510	0.336	15.578
278	cg19084031	15	38361362		0.501	0.164	0.337	31.541
279	cg10957001	12	99118507	APAF1; APAF1; APAF1; APAF1; APAF1	0.878	0.537	0.341	23.095
280	cg04499455	6	31356802		0.652	0.311	0.341	14.858
281	cg14889167	5	132925337	FSTL4	0.516	0.172	0.344	16.077
282	cg27153751	21	43869662		0.688	0.344	0.344	15.652
283	cg25641515	12	132965879		0.673	0.328	0.346	28.702
284	cg08103988	17	6558365		0.828	0.481	0.347	18.111
285	cg13117582	17	81025461		0.959	0.612	0.348	17.933
286	cg01081438	1	92417998	BRDT; BRDT	0.768	0.415	0.352	17.421
287	cg23893060	22	45498115		0.834	0.478	0.356	15.586
288	cg16917903	18	722818	YES1	0.870	0.512	0.359	13.794
289	cg13905298	5	141485167		0.401	0.041	0.359	27.215
290	cg08210706	14	95046686	SERPINA5	0.855	0.493	0.362	15.596

(Cont. Supplementary Table 2)

Serial number	CpG site ID	Chromosome	Position	UCSC_RefGene_Name	AVG_Beta in patients	AVG_Beta in controls	Delta Beta	DiffScore
291	cg22071943	5	1225434	SLC6A18	0.699	0.335	0.363	14.148
292	cg05327255	6	101294430	ASCC3; ASCC3	0.900	0.534	0.366	21.816
293	cg09829645	2	71723690	DYSF; DYSF; DYSF; DYSF; DYSF; DYSF; DYSF; DYSF; DYSF; DYSF; DYSF; DYSF; DYSF	0.731	0.363	0.368	25.478
294	cg06150107	2	235884005	SH3BP4	0.661	0.291	0.370	14.911
295	cg23213876	1	53924164	DMRTB1	0.846	0.468	0.378	30.630
296	cg13232075	1	204556835		0.662	0.283	0.379	15.539
297	cg14152758	13	110954169	COL4A1; COL4A1	0.693	0.311	0.382	26.694
298	cg05526809	4	1309416	MAEA; MAEA	0.764	0.381	0.383	17.549
299	cg06631775	12	132972807		0.729	0.345	0.384	13.794
300	cg02448536	1	204561617		0.889	0.505	0.384	18.467
301	cg23854988	22	45330438	PHF21B; PHF21B; PHF21B; PHF21B	0.756	0.368	0.388	15.039
303	cg17365896	15	38423730		0.769	0.377	0.392	18.738
304	cg11920595	10	104373903	SUFU; SUFU	0.502	0.108	0.395	23.040
305	cg14763408	4	38777471	TLR10; TLR10; TLR10; TLR10; TLR10	0.875	0.480	0.395	19.646
306	cg23681001	1	53936382		0.795	0.399	0.396	35.989
307	cg21234342	6	46871130	GPR116; GPR116	0.825	0.429	0.396	19.010
308	cg02171206	16	78512543	WWOX; WWOX	0.647	0.249	0.398	17.247
309	cg00730761	6	101113084	ASCC3	0.446	0.039	0.406	23.416
310	cg12171675	19	15083795	SLC1A6	0.937	0.528	0.408	25.018
311	cg01445689	7	158703106	WDR60	0.940	0.528	0.412	18.818
312	cg05904344	13	113843426	PCID2; PCID2; PCID2; PCID2; PCID2	0.870	0.449	0.421	21.231
313	cg13038767	12	67989361		0.656	0.230	0.426	18.908
314	cg17534070	5	168195355	SLIT3; MIR218-2	0.719	0.281	0.438	15.615
315	cg17395184	15	42750462	ZFP106	0.830	0.390	0.439	26.550
316	cg23855802	15	100543352	ADAMTS17	0.679	0.235	0.444	24.574
317	cg10769535	1	172115154	DNM3; DNM3; MIR199A2	0.860	0.415	0.445	17.554
318	cg14780957	22	45257245	PRR5-ARHGAP8; ARHGAP8; ARHGAP8; ARHGAP8	0.918	0.460	0.458	18.578
319	cg23996696	21	31322913		0.702	0.235	0.467	19.602
320	cg02218418	5	156938326	ADAM19	0.763	0.284	0.479	23.332
321	cg25710745	5	36683903	SLC1A3; SLC1A3; SLC1A3; SLC1A3	0.884	0.354	0.529	26.269

Supplementary Table 3. Changed methylation sites were assigned to 168 known gene regions

Serial number	UCSC_RefGene_Name	Serial number	UCSC_RefGene_Name	Serial number	UCSC_RefGene_Name	Serial number	UCSC_RefGene_Name	Serial number	UCSC_RefGene_Name
1	C3orf50	35	HLA-H	69	DLGAP1	103	LINC00578	137	DLG3
2	HEATR2	36	CARS2	70	ATP2C1	104	RNF213	138	GLP2R
3	B3GLCT	37	GNA15	71	ZDHHC4	105	OSBPL5	139	NID1
4	TAGLN3	38	ANGPT2	72	PTPRN2	106	HLA-A	140	RHCE
5	KIAA1026	39	IFRD1	73	MCM2	107	MCF2L	141	PROZ
6	CLDN4	40	MSC-AS1	74	INPP5B	108	SLC15A4	142	ADRA1B
7	PSTPIP2	41	LINC00504	75	C10orf47	109	KRT23	143	ADPRHL1
8	MEOX2	42	TTC23	76	KLK9	110	MYOM2	144	SPRED2
9	ROBO1	43	TRAK2	77	LOC101927730	111	RABGAP1L	145	FSTL4
10	PPP1R16B	44	NCKIPSD	78	TNFSF8	112	MAPK10	146	YES1
11	BRDT	45	FOXK1	79	ASTL	113	ZNF611	147	SERPINA5
12	RNU6-71P	46	PRKCZ	80	PLD6	114	SPAG1	148	SLC6A18
13	COL6A2	47	SORCS1	81	KIRREL3	115	HCG9	149	DYSF
14	ABHD12	48	RNASEN	82	SLC6A12	116	PTPRS	150	SH3BP4
15	SULF2	49	SNX26	83	MYT1L	117	LCT	151	DMRTB1
16	TANC1	50	CHML	84	IL17RA	118	GZMK	152	COL4A1
17	PTGES	51	PGBD5	85	LDB3	119	FEZ2	153	MAEA
18	ALS2CR12	52	PSD	86	SLC12A7	120	DUSP27	154	PHF21B
19	ABI1	53	SNTG2	87	OSBPL10	121	COPB1	155	SUFU
20	MPPED1	54	ABCC9	88	CCR2	122	ST8SIA5	156	TLR10
21	PFKP	55	FAM101A	89	LINC01252	123	BNIP3	157	GPR116
22	UBE2E2	56	CNST	90	ODZ2	124	MPPED2	158	WWOX
23	USP6NL	57	ARID1B	91	PITRM1	125	UBA5	159	SLC1A6
24	LINC01307	58	COPS4	92	CYFIP1	126	C3orf20	160	WDR60
25	APAF1	59	ERLIN1	93	SRPK3	127	CYFIP2	161	PCID2
26	BCAR3	60	INADL	94	SORCS2	128	TLR6	162	SLIT3
27	RAB1A	61	GFPT2	95	CPNE4	129	NSF	163	ZFP106
28	LONRF2	62	LAPTM5	96	TNXB	130	GCK	164	ADAMTS17
29	FOLH1	63	LOC101928358	97	ATP8A2	131	STXBP5-AS1	165	DNM3
30	ADCK2	64	DOK6	98	INPP5A	132	RASA3	166	ARHGAP8
31	MCC	65	GPR65	99	IFT140	133	SLC25A21	167	ADAM19
32	EYA4	66	NOTCH4	100	SH3D19	134	ZNF83	168	SLC1A3
33	PUM1	67	ASCC3	101	CTSB	135	TIMP2		
34	OR4L1	68	C14orf126	102	NRG3	136	ADAM3A		

Supplementary Table 4. Gene ontology enrichment analysis results of differentially methylated genes

Term_ID	Term_description	Term_url	Fold Enrichment	Genes	GeneSymbols	*P*_value	-log10 (*p* value)	FDR_bh
GO:0070100	negative regulation of chemokine-mediated signaling pathway	http://amigo.geneontology.org/amigo/term/GO:0070100	46.052	6091; 6586	ROBO1; SLIT3	0.002	2.812	0.197
GO:0038096	Fc-gamma receptor signaling pathway involved in phagocytosis	http://amigo.geneontology.org/amigo/term/GO:0038096	6.257	51517; 23191; 7525; 10006; 26999	NCKIPSD; CYFIP1; YES1; ABI1; CYFIP2	0.002	2.767	0.197
GO:0051346	negative regulation of hydrolase activity	http://amigo.geneontology.org/amigo/term/GO:0051346	38.377	5590; 5104	PRKCZ; SERPINA5	0.002	2.689	0.197
GO:2000667	positive regulation of interleukin-13 secretion	http://amigo.geneontology.org/amigo/term/GO:2000667	38.377	23765; 5590	IL17RA; PRKCZ	0.002	2.689	0.197
GO:0048671	negative regulation of collateral sprouting	http://amigo.geneontology.org/amigo/term/GO:0048671	38.377	23105; 3475	FSTL4; IFRD1	0.002	2.689	0.197
GO:0002224	toll-like receptor signaling pathway	http://amigo.geneontology.org/amigo/term/GO:0002224	12.792	81793; 1508; 10333	TLR10; CTSB; TLR6	0.002	2.646	0.197
GO:0009611	response to wounding	http://amigo.geneontology.org/amigo/term/GO:0009611	7.550	55959; 6507; 11202; 729230	SULF2; SLC1A3; KLK8; CCR2	0.003	2.587	0.197
GO:0048705	skeletal system morphogenesis	http://amigo.geneontology.org/amigo/term/GO:0048705	11.513	9742; 144347; 51741	IFT140; FAM101A; WWOX	0.003	2.526	0.197
GO:0071711	basement membrane organization	http://amigo.geneontology.org/amigo/term/GO:0071711	28.783	4811; 1282	NID1; COL4A1	0.003	2.488	0.197
GO:0006002	fructose 6-phosphate metabolic process	http://amigo.geneontology.org/amigo/term/GO:0006002	28.783	5214; 9945	PFKP; GFPT2	0.003	2.488	0.197
GO:0002480	antigen processing and presentation of exogenous peptide antigen via MHC class I, TAP-independent	http://amigo.geneontology.org/amigo/term/GO:0002480	25.585	3136; 3105	HLA-H; HLA-A	0.004	2.404	0.197
GO:0010996	response to auditory stimulus	http://amigo.geneontology.org/amigo/term/GO:0010996	25.585	51761; 26090	ATP8A2; ABHD12	0.004	2.404	0.197
GO:0032836	glomerular basement membrane development	http://amigo.geneontology.org/amigo/term/GO:0032836	25.585	4811; 55959	NID1; SULF2	0.004	2.404	0.197
GO:0007165	signal transduction	http://amigo.geneontology.org/amigo/term/GO:0007165	2.056	8412; 5590; 10060; 10333; 51517; 51684; 9536; 9637; 3633; 22821; 23779; 285; 5602; 944; 8471; 5662; 4163; 1364; 27032	BCAR3; PRKCZ; ABCC9; TLR6; NCKIPSD; SUFU; PTGES; FEZ2; INPP5B; RASA3; ARHGAP8; ANGPT2; MAPK10; TNFSF8; IRS4; PSD; MCC; CLDN4; ATP2C1	0.005	2.315	0.216
GO:0050707	regulation of cytokine secretion	http://amigo.geneontology.org/amigo/term/GO:0050707	20.933	81793; 10333	TLR10; TLR6	0.006	2.257	0.216
GO:0019068	virion assembly	http://amigo.geneontology.org/amigo/term/GO:0019068	20.933	9712; 5861	USP6NL; RAB1A	0.006	2.257	0.216
GO:0090630	activation of GTPase activity	http://amigo.geneontology.org/amigo/term/GO:0090630	5.981	9712; 8477; 9910; 113622	USP6NL; GPR65; RABGAP1L; ADPRHL1	0.006	2.245	0.216
GO:0007268	chemical synaptic transmission	http://amigo.geneontology.org/amigo/term/GO:0007268	3.429	10723; 6507; 9229; 6539; 6511; 5802; 1741	SLC12A7; SLC1A3; DLGAP1; SLC6A12; SLC1A6; PTPRS; DLG3	0.006	2.223	0.216
GO:0035385	Roundabout signaling pathway	http://amigo.geneontology.org/amigo/term/GO:0035385	19.189	6091; 6586	ROBO1; SLIT3	0.006	2.192	0.218
GO:0031338	regulation of vesicle fusion	http://amigo.geneontology.org/amigo/term/GO:0031338	8.424	9712; 9910; 113622	USP6NL; RABGAP1L; ADPRHL1	0.007	2.172	0.218
GO:0089711	L-glutamate transmembrane transport	http://amigo.geneontology.org/amigo/term/GO:0089711	17.712	6507; 6511	SLC1A3; SLC1A6	0.007	2.133	0.227
GO:0047496	vesicle transport along microtubule	http://amigo.geneontology.org/amigo/term/GO:0047496	16.447	5861; 5590	RAB1A; PRKCZ	0.008	2.077	0.246
GO:0031532	actin cytoskeleton reorganization	http://amigo.geneontology.org/amigo/term/GO:0031532	7.349	8477; 5590; 27032	GPR65; PRKCZ; ATP2C1	0.010	2.019	0.262

(Cont. Supplementary Table 4)

Term_ID	Term_description	Term_url	Fold Enrichment	Genes	GeneSymbols	*P*_value	-log10 (*p* value)	FDR_bh
GO:0006508	proteolysis	http://amigo.geneontology.org/amigo/term/GO:0006508	2.508	431705; 3003; 10531; 51684; 170691; 2346; 164832; 1508; 284366; 11202	ASTL; GZMK; PITRM1; SUFU; ADAMTS17; FOLH1; LONRF2; CTSB; KLK9; KLK8	0.010	2.013	0.262
GO:0009416	response to light stimulus	http://amigo.geneontology.org/amigo/term/GO:0009416	14.391	5602; 6507	MAPK10; SLC1A3	0.011	1.977	0.265
GO:0071560	cellular response to transforming growth factor beta stimulus	http://amigo.geneontology.org/amigo/term/GO:0071560	7.049	51741; 317; 7525	WWOX; APAF1; YES1	0.011	1.973	0.265
GO:0006886	intracellular protein transport	http://amigo.geneontology.org/amigo/term/GO:0006886	3.353	4905; 9712; 1122; 9910; 1315; 113622	NSF; USP6NL; CHML; RABGAP1L; COPB1; ADPRHL1	0.012	1.937	0.278
GO:0007399	nervous system development	http://amigo.geneontology.org/amigo/term/GO:0007399	2.909	9637; 23040; 57492; 317; 744; 1741; 6091	FEZ2; MYT1L; ARID1B; APAF1; MPPED2; DLG3; ROBO1	0.014	1.869	0.307
GO:0050790	regulation of catalytic activity	http://amigo.geneontology.org/amigo/term/GO:0050790	6.280	26051; 1508; 23677	PPP1R16B; CTSB; SH3BP4	0.014	1.845	0.307
GO:0006811	ion transport	http://amigo.geneontology.org/amigo/term/GO:0006811	4.386	121260; 10723; 6507; 6511	SLC15A4; SLC12A7; SLC1A3; SLC1A6	0.016	1.805	0.307
GO:0046856	phosphatidylinositol dephosphorylation	http://amigo.geneontology.org/amigo/term/GO:0046856	10.011	3633; 3632	INPP5B; INPP5A	0.020	1.702	0.307
GO:0030574	collagen catabolic process	http://amigo.geneontology.org/amigo/term/GO:0030574	5.397	1282; 1508; 1292	COL4A1; CTSB; COL6A2	0.021	1.679	0.307
GO:0006836	neurotransmitter transport	http://amigo.geneontology.org/amigo/term/GO:0006836	9.594	6539; 348932	SLC6A12; SLC6A18	0.021	1.670	0.307
GO:0046580	negative regulation of Ras protein signal transduction	http://amigo.geneontology.org/amigo/term/GO:0046580	9.210	22821; 7077	RASA3; TIMP2	0.023	1.639	0.307
GO:0003333	amino acid transmembrane transport	http://amigo.geneontology.org/amigo/term/GO:0003333	9.210	6539; 348932	SLC6A12; SLC6A18	0.023	1.639	0.307
GO:0006891	intra-Golgi vesicle-mediated transport	http://amigo.geneontology.org/amigo/term/GO:0006891	8.856	4905; 1315	NSF; COPB1	0.025	1.609	0.307
GO:0061621	canonical glycolysis	http://amigo.geneontology.org/amigo/term/GO:0061621	8.856	2645; 5214	GCK; PFKP	0.025	1.609	0.307
GO:0048010	vascular endothelial growth factor receptor signaling pathway	http://amigo.geneontology.org/amigo/term/GO:0048010	4.865	23191; 10006; 26999	CYFIP1; ABI1; CYFIP2	0.027	1.567	0.307
GO:0001569	patterning of blood vessels	http://amigo.geneontology.org/amigo/term/GO:0001569	8.224	1282; 4855	COL4A1; NOTCH4	0.028	1.553	0.307
GO:0014047	glutamate secretion	http://amigo.geneontology.org/amigo/term/GO:0014047	8.224	6507; 6511	SLC1A3; SLC1A6	0.028	1.553	0.307
GO:0002474	antigen processing and presentation of peptide antigen via MHC class I	http://amigo.geneontology.org/amigo/term/GO:0002474	7.940	3136; 3105	HLA-H; HLA-A	0.030	1.527	0.307
GO:0051402	neuron apoptotic process	http://amigo.geneontology.org/amigo/term/GO:0051402	7.428	317; 664	APAF1; BNIP3	0.033	1.477	0.307
GO:0006890	retrograde vesicle-mediated transport, Golgi to ER	http://amigo.geneontology.org/amigo/term/GO:0006890	4.428	4905; 5861; 1315	NSF; RAB1A; COPB1	0.034	1.467	0.307
GO:0002755	MyD88-dependent toll-like receptor signaling pathway	http://amigo.geneontology.org/amigo/term/GO:0002755	7.196	81793; 10333	TLR10; TLR6	0.035	1.453	0.307
GO:0043588	skin development	http://amigo.geneontology.org/amigo/term/GO:0043588	6.978	51761; 51684	ATP8A2; SUFU	0.037	1.430	0.307
GO:0015758	glucose transport	http://amigo.geneontology.org/amigo/term/GO:0015758	6.978	2645; 7525	GCK; YES1	0.037	1.430	0.307
GO:0006865	amino acid transport	http://amigo.geneontology.org/amigo/term/GO:0006865	6.772	6539; 348932	SLC6A12; SLC6A18	0.039	1.407	0.307
GO:1902017	regulation of cilium assembly	http://amigo.geneontology.org/amigo/term/GO:1902017	6.396	9712; 9742	USP6NL; IFT140	0.043	1.365	0.307

(Cont. Supplementary Table 4)

Term_ID	Term_description	Term_url	Fold Enrichment	Genes	GeneSymbols	*P*_value	-log10 (*p* value)	FDR_bh
GO:0007188	adenylate cyclase-modulating G-protein coupled receptor signaling pathway	http://amigo.geneontology.org/amigo/term/GO:0007188	6.396	9340; 147	GLP2R; ADRA1B	0.043	1.365	0.307
GO:0019882	antigen processing and presentation	http://amigo.geneontology.org/amigo/term/GO:0019882	6.223	3136; 3105	HLA-H; HLA-A	0.045	1.344	0.307
GO:0008219	cell death	http://amigo.geneontology.org/amigo/term/GO:0008219	6.223	11202; 664	KLK8; BNIP3	0.045	1.344	0.307
GO:0030154	cell differentiation	http://amigo.geneontology.org/amigo/term/GO:0030154	2.093	676; 2070; 23040; 7525; 4855; 221937; 317; 26576	BRDT; EYA4; MYT1L; YES1; NOTCH4; FOXK1; APAF1; SRPK3	0.046	1.337	0.307
GO:0010508	positive regulation of autophagy	http://amigo.geneontology.org/amigo/term/GO:0010508	5.904	664; 23677	BNIP3; SH3BP4	0.050	1.305	0.307

Supplementary Table 5. Gene ontology enrichment analysis results for genes of the different sites near transcription start site

Term_ID	Term_description	Term_url	Fold Enrichment	Genes	GeneSymbols	*P*_value	-log10 (*p* value)	FDR_bh
GO:0051346	negative regulation of hydrolase activity	http://amigo.geneontology.org/amigo/term/GO:0051346	191.885	5590; 5104	PRKCZ; SERPINA5	9.24E-5	4.034	0.017
GO:0009611	response to wounding	http://amigo.geneontology.org/amigo/term/GO:0009611	28.311	11202; 55959; 729230	KLK8; SULF2; CCR2	0.000	3.616	0.023
GO:0031532	actin cytoskeleton reorganization	http://amigo.geneontology.org/amigo/term/GO:0031532	24.496	8477; 5590	GPR65; PRKCZ	0.004	2.434	0.103
GO:0006955	immune response	http://amigo.geneontology.org/amigo/term/GO:0006955	6.753	3136; 8477; 944; 729230	HLA-H; GPR65; TNFSF8; CCR2	0.004	2.374	0.103
GO:0016525	negative regulation of angiogenesis	http://amigo.geneontology.org/amigo/term/GO:0016525	19.514	285; 729230	ANGPT2; CCR2	0.006	2.248	0.103
GO:0008286	insulin receptor signaling pathway	http://amigo.geneontology.org/amigo/term/GO:0008286	14.952	5590; 8471	PRKCZ; IRS4	0.009	2.032	0.103
GO:0002829	negative regulation of type 2 immune response	http://amigo.geneontology.org/amigo/term/GO:0002829	115.131	729230	CCR2	0.011	1.970	0.103
GO:0035860	glial cell-derived neurotrophic factor receptor signaling pathway	http://amigo.geneontology.org/amigo/term/GO:0035860	115.131	55959	SULF2	0.011	1.970	0.103
GO:0043374	CD8-positive, alpha-beta T cell differentiation	http://amigo.geneontology.org/amigo/term/GO:0043374	115.131	944	TNFSF8	0.011	1.970	0.103
GO:0031584	activation of phospholipase D activity	http://amigo.geneontology.org/amigo/term/GO:0031584	95.943	5590	PRKCZ	0.012	1.904	0.103
GO:2000553	positive regulation of T-helper 2 cell cytokine production	http://amigo.geneontology.org/amigo/term/GO:2000553	95.943	5590	PRKCZ	0.012	1.904	0.103
GO:2000667	positive regulation of interleukin-13 secretion	http://amigo.geneontology.org/amigo/term/GO:2000667	95.943	5590	PRKCZ	0.012	1.904	0.103
GO:0032020	ISG15-protein conjugation	http://amigo.geneontology.org/amigo/term/GO:0032020	95.943	7325	UBE2E2	0.012	1.904	0.103
GO:0018344	protein geranylgeranylation	http://amigo.geneontology.org/amigo/term/GO:0018344	95.943	1122	CHML	0.012	1.904	0.103
GO:0048671	negative regulation of collateral sprouting	http://amigo.geneontology.org/amigo/term/GO:0048671	95.943	3475	IFRD1	0.012	1.904	0.103
GO:0048681	negative regulation of axon regeneration	http://amigo.geneontology.org/amigo/term/GO:0048681	95.943	11202	KLK8	0.012	1.904	0.103
GO:0015813	L-glutamate transport	http://amigo.geneontology.org/amigo/term/GO:0015813	82.236	6511	SLC1A6	0.014	1.846	0.103
GO:0031642	negative regulation of myelination	http://amigo.geneontology.org/amigo/term/GO:0031642	82.236	11202	KLK8	0.014	1.846	0.103
GO:0032049	cardiolipin biosynthetic process	http://amigo.geneontology.org/amigo/term/GO:0032049	71.957	201164	PLD6	0.016	1.795	0.103
GO:0002827	positive regulation of T-helper 1 type immune response	http://amigo.geneontology.org/amigo/term/GO:0002827	71.957	729230	CCR2	0.016	1.795	0.103
GO:0045630	positive regulation of T-helper 2 cell differentiation	http://amigo.geneontology.org/amigo/term/GO:0045630	71.957	5590	PRKCZ	0.016	1.795	0.103
GO:0010954	positive regulation of protein processing	http://amigo.geneontology.org/amigo/term/GO:0010954	71.957	431705	ASTL	0.016	1.795	0.103
GO:0007165	signal transduction	http://amigo.geneontology.org/amigo/term/GO:0007165	3.246	5590; 285; 5602; 944; 8471; 1364	PRKCZ; ANGPT2; MAPK10; TNFSF8; IRS4; CLDN4	0.017	1.772	0.103
GO:0002480	antigen processing and presentation of exogenous peptide antigen via MHC class I, TAP-independent	http://amigo.geneontology.org/amigo/term/GO:0002480	63.962	3136	HLA-H	0.018	1.750	0.103
GO:0050807	regulation of synapse organization	http://amigo.geneontology.org/amigo/term/GO:0050807	63.962	11202	KLK8	0.018	1.750	0.103
GO:0010388	cullin deneddylation	http://amigo.geneontology.org/amigo/term/GO:0010388	63.962	51138	COPS4	0.018	1.750	0.103
GO:0046641	positive regulation of alpha-beta T cell proliferation	http://amigo.geneontology.org/amigo/term/GO:0046641	63.962	729230	CCR2	0.018	1.750	0.103

(Cont. Supplementary Table 5)

Term_ID	Term_description	Term_url	Fold Enrichment	Genes	GeneSymbols	*P*_value	-log10 (*p* value)	FDR_bh
GO:0032836	glomerular basement membrane development	http://amigo.geneontology.org/amigo/term/GO:0032836	63.962	55959	SULF2	0.018	1.750	0.103
GO:0003094	glomerular filtration	http://amigo.geneontology.org/amigo/term/GO:0003094	57.566	55959	SULF2	0.020	1.709	0.103
GO:0040037	negative regulation of fibroblast growth factor receptor signaling pathway	http://amigo.geneontology.org/amigo/term/GO:0040037	57.566	55959	SULF2	0.020	1.709	0.103
GO:0030517	negative regulation of axon extension	http://amigo.geneontology.org/amigo/term/GO:0030517	57.566	3475	IFRD1	0.020	1.709	0.103
GO:0010820	positive regulation of T cell chemotaxis	http://amigo.geneontology.org/amigo/term/GO:0010820	57.566	729230	CCR2	0.020	1.709	0.103
GO:0050732	negative regulation of peptidyl-tyrosine phosphorylation	http://amigo.geneontology.org/amigo/term/GO:0050732	52.332	5590	PRKCZ	0.021	1.671	0.103
GO:0035413	positive regulation of catenin import into nucleus	http://amigo.geneontology.org/amigo/term/GO:0035413	52.332	55959	SULF2	0.021	1.671	0.103
GO:0060081	membrane hyperpolarization	http://amigo.geneontology.org/amigo/term/GO:0060081	52.332	5590	PRKCZ	0.021	1.671	0.103
GO:0042535	positive regulation of tumor necrosis factor biosynthetic process	http://amigo.geneontology.org/amigo/term/GO:0042535	52.332	729230	CCR2	0.021	1.671	0.103
GO:0010447	response to acidic pH	http://amigo.geneontology.org/amigo/term/GO:0010447	47.971	8477	GPR65	0.023	1.637	0.103
GO:0007342	fusion of sperm to egg plasma membrane	http://amigo.geneontology.org/amigo/term/GO:0007342	47.971	5104	SERPINA5	0.023	1.637	0.103
GO:0019725	cellular homeostasis	http://amigo.geneontology.org/amigo/term/GO:0019725	47.971	729230	CCR2	0.023	1.637	0.103
GO:0043616	keratinocyte proliferation	http://amigo.geneontology.org/amigo/term/GO:0043616	47.971	11202	KLK8	0.023	1.637	0.103
GO:0043403	skeletal muscle tissue regeneration	http://amigo.geneontology.org/amigo/term/GO:0043403	44.281	3475	IFRD1	0.025	1.605	0.103
GO:0089711	L-glutamate transmembrane transport	http://amigo.geneontology.org/amigo/term/GO:0089711	44.281	6511	SLC1A6	0.025	1.605	0.103
GO:0046628	positive regulation of insulin receptor signaling pathway	http://amigo.geneontology.org/amigo/term/GO:0046628	44.281	5590	PRKCZ	0.025	1.605	0.103
GO:0032743	positive regulation of interleukin-2 production	http://amigo.geneontology.org/amigo/term/GO:0032743	41.118	729230	CCR2	0.027	1.576	0.103
GO:0047496	vesicle transport along microtubule	http://amigo.geneontology.org/amigo/term/GO:0047496	41.118	5590	PRKCZ	0.027	1.576	0.103
GO:0002063	chondrocyte development	http://amigo.geneontology.org/amigo/term/GO:0002063	41.118	55959	SULF2	0.027	1.576	0.103
GO:0043537	negative regulation of blood vessel endothelial cell migration	http://amigo.geneontology.org/amigo/term/GO:0043537	41.118	285	ANGPT2	0.027	1.576	0.103
GO:0010812	negative regulation of cell-substrate adhesion	http://amigo.geneontology.org/amigo/term/GO:0010812	41.118	285	ANGPT2	0.027	1.576	0.103
GO:0090026	positive regulation of monocyte chemotaxis	http://amigo.geneontology.org/amigo/term/GO:0090026	38.377	729230	CCR2	0.028	1.548	0.104
GO:0034587	piRNA metabolic process	http://amigo.geneontology.org/amigo/term/GO:0034587	38.377	201164	PLD6	0.028	1.548	0.104
GO:0070528	protein kinase C signaling	http://amigo.geneontology.org/amigo/term/GO:0070528	38.377	5590	PRKCZ	0.028	1.548	0.104
GO:1990138	neuron projection extension	http://amigo.geneontology.org/amigo/term/GO:1990138	35.978	5590	PRKCZ	0.030	1.522	0.104
GO:0009416	response to light stimulus	http://amigo.geneontology.org/amigo/term/GO:0009416	35.978	5602	MAPK10	0.030	1.522	0.104
GO:0002407	dendritic cell chemotaxis	http://amigo.geneontology.org/amigo/term/GO:0002407	35.978	729230	CCR2	0.030	1.522	0.104

(Cont. Supplementary Table 5)

Term_ID	Term_description	Term_url	Fold Enrichment	Genes	GeneSymbols	*P*_value	-log10 (*p* value)	FDR_bh
GO:0031333	negative regulation of protein complex assembly	http://amigo.geneontology.org/amigo/term/GO:0031333	33.862	5590	PRKCZ	0.032	1.498	0.104
GO:0061436	establishment of skin barrier	http://amigo.geneontology.org/amigo/term/GO:0061436	33.862	1364	CLDN4	0.032	1.498	0.104
GO:0043046	DNA methylation involved in gamete generation	http://amigo.geneontology.org/amigo/term/GO:0043046	31.981	201164	PLD6	0.034	1.475	0.104
GO:0060384	innervation	http://amigo.geneontology.org/amigo/term/GO:0060384	31.981	55959	SULF2	0.034	1.475	0.104
GO:0050870	positive regulation of T cell activation	http://amigo.geneontology.org/amigo/term/GO:0050870	31.981	729230	CCR2	0.034	1.475	0.104
GO:0008053	mitochondrial fusion	http://amigo.geneontology.org/amigo/term/GO:0008053	31.981	201164	PLD6	0.034	1.475	0.104
GO:2000463	positive regulation of excitatory postsynaptic potential	http://amigo.geneontology.org/amigo/term/GO:2000463	28.783	5590	PRKCZ	0.037	1.432	0.109
GO:0032753	positive regulation of interleukin-4 production	http://amigo.geneontology.org/amigo/term/GO:0032753	28.783	5590	PRKCZ	0.037	1.432	0.109
GO:1900087	positive regulation of G1/S transition of mitotic cell cycle	http://amigo.geneontology.org/amigo/term/GO:1900087	28.783	7325	UBE2E2	0.037	1.432	0.109
GO:0016338	calcium-independent cell-cell adhesion via plasma membrane cell-adhesion molecules	http://amigo.geneontology.org/amigo/term/GO:0016338	27.412	1364	CLDN4	0.039	1.412	0.109
GO:0001954	positive regulation of cell-matrix adhesion	http://amigo.geneontology.org/amigo/term/GO:0001954	27.412	5590	PRKCZ	0.039	1.412	0.109
GO:0007194	negative regulation of adenylate cyclase activity	http://amigo.geneontology.org/amigo/term/GO:0007194	26.166	729230	CCR2	0.040	1.393	0.109
GO:0007548	sex differentiation	http://amigo.geneontology.org/amigo/term/GO:0007548	26.166	63948	DMRTB1	0.040	1.393	0.109
GO:0000715	nucleotide-excision repair, DNA damage recognition	http://amigo.geneontology.org/amigo/term/GO:0000715	25.028	51138	COPS4	0.042	1.375	0.109
GO:0051899	membrane depolarization	http://amigo.geneontology.org/amigo/term/GO:0051899	23.986	5590	PRKCZ	0.044	1.358	0.109
GO:0006836	neurotransmitter transport	http://amigo.geneontology.org/amigo/term/GO:0006836	23.986	348932	SLC6A18	0.044	1.358	0.109
GO:0060135	maternal process involved in female pregnancy	http://amigo.geneontology.org/amigo/term/GO:0060135	23.986	285	ANGPT2	0.044	1.358	0.109
GO:0030010	establishment of cell polarity	http://amigo.geneontology.org/amigo/term/GO:0030010	23.986	5590	PRKCZ	0.044	1.358	0.109
GO:0007126	meiotic nuclear division	http://amigo.geneontology.org/amigo/term/GO:0007126	23.986	201164	PLD6	0.044	1.358	0.109
GO:0051090	regulation of sequence-specific DNA binding transcription factor activity	http://amigo.geneontology.org/amigo/term/GO:0051090	23.026	5602	MAPK10	0.046	1.341	0.109
GO:0003333	amino acid transmembrane transport	http://amigo.geneontology.org/amigo/term/GO:0003333	23.026	348932	SLC6A18	0.046	1.341	0.109
GO:0010575	positive regulation of vascular endothelial growth factor production	http://amigo.geneontology.org/amigo/term/GO:0010575	22.141	55959	SULF2	0.047	1.325	0.109
GO:0019216	regulation of lipid metabolic process	http://amigo.geneontology.org/amigo/term/GO:0019216	22.141	8471	IRS4	0.047	1.325	0.109
GO:0007616	long-term memory	http://amigo.geneontology.org/amigo/term/GO:0007616	22.141	5590	PRKCZ	0.047	1.325	0.109
GO:0032148	activation of protein kinase B activity	http://amigo.geneontology.org/amigo/term/GO:0032148	22.141	5590	PRKCZ	0.047	1.325	0.109
GO:0097421	liver regeneration	http://amigo.geneontology.org/amigo/term/GO:0097421	21.321	55959	SULF2	0.049	1.310	0.109
GO:0070979	protein K11-linked ubiquitination	http://amigo.geneontology.org/amigo/term/GO:0070979	21.321	7325	UBE2E2	0.049	1.310	0.109

Supplementary Table 6. Kyoto Encyclopedia of Genes and Genomes pathway analysis results of differentially methylated genes

Term_ID	Term_description	Term_url	Fold Enrichment	Genes	Gene Symbols	*P*_value	-log10 (*p* value)	FDR_bh
path:hsa04930	Type II diabetes mellitus	http://www.kegg.jp/kegg-bin/show_pathway?hsa04930/2645%09yellow/5602%09yellow/5590%09yellow/8471%09yellow	10.240	2645; 5602; 5590; 8471	GCK; MAPK10; PRKCZ; IRS4	0.001	3.012	0.136
path:hsa00052	Galactose metabolism	http://www.kegg.jp/kegg-bin/show_pathway?hsa00052/2645%09yellow/3938%09yellow/5214%09yellow	11.892	2645; 3938; 5214	GCK; LCT; PFKP	0.003	2.545	0.200
path:hsa05134	Legionellosis	http://www.kegg.jp/kegg-bin/show_pathway?hsa05134/317%09yellow/5861%09yellow/664%09yellow	6.703	317; 5861; 664	APAF1; RAB1A; BNIP3	0.013	1.899	0.589
path:hsa04530	Tight junction	http://www.kegg.jp/kegg-bin/show_pathway?hsa04530/10207%09yellow/1364%09yellow/5590%09yellow/7525%09yellow	3.536	10207; 1364; 5590; 7525	INADL; CLDN4; PRKCZ; YES1	0.032	1.489	0.657
path:hsa04910	Insulin signaling pathway	http://www.kegg.jp/kegg-bin/show_pathway?hsa04910/2645%09yellow/5602%09yellow/5590%09yellow/8471%09yellow	3.511	2645; 5602; 5590; 8471	GCK; MAPK10; PRKCZ; IRS4	0.033	1.480	0.657
path:hsa04215	Apoptosis - multiple species	http://www.kegg.jp/kegg-bin/show_pathway?hsa04215/5602%09yellow/317%09yellow	7.447	5602; 317	MAPK10; APAF1	0.034	1.470	0.657
path:hsa04512	ECM-receptor interaction	http://www.kegg.jp/kegg-bin/show_pathway?hsa04512/7148%09yellow/1282%09yellow/1292%09yellow	4.496	7148; 1282; 1292	TNXB; COL4A1; COL6A2	0.034	1.467	0.657
path:hsa00250	Alanine, aspartate and glutamate metabolism	http://www.kegg.jp/kegg-bin/show_pathway?hsa00250/2346%09yellow/9945%09yellow	7.022	2346; 9945	FOLH1; GFPT2	0.038	1.426	0.657
path:hsa00524	Neomycin, kanamycin and gentamicin biosynthesis	http://www.kegg.jp/kegg-bin/show_pathway?hsa00524/2645%09yellow	24.576	2645	GCK	0.048	1.317	0.668

Supplementary Table 7. Kyoto Encyclopedia of Genes and Genomes pathway analysis results of genes of the different sites near transcription start site

Term_ID	Term_description	Term_url	Fold Enrichment	Genes	Gene Symbols	*P*_value	-log10 (*p* value)	FDR_bh
path:hsa04930	Type II diabetes mellitus	http://www.kegg.jp/kegg-bin/show_pathway?hsa04930/5602%09yellow/5590%09yellow/8471%09yellow	34.264	5602; 5590; 8471	MAPK10; PRKCZ; IRS4	0.000	3.754	0.012
path:hsa04910	Insulin signaling pathway	http://www.kegg.jp/kegg-bin/show_pathway?hsa04910/5602%09yellow/5590%09yellow/8471%09yellow	11.748	5602; 5590; 8471	MAPK10; PRKCZ; IRS4	0.003	2.463	0.119
path:hsa04920	Adipocytokine signaling pathway	http://www.kegg.jp/kegg-bin/show_pathway?hsa04920/5602%09yellow/8471%09yellow	15.664	5602; 8471	MAPK10; IRS4	0.009	2.023	0.218
path:hsa04933	AGE-RAGE signaling pathway in diabetic complications	http://www.kegg.jp/kegg-bin/show_pathway?hsa04933/5602%09yellow/5590%09yellow	10.856	5602; 5590	MAPK10; PRKCZ	0.019	1.730	0.254
path:hsa04931	Insulin resistance	http://www.kegg.jp/kegg-bin/show_pathway?hsa04931/5602%09yellow/5590%09yellow	10.059	5602; 5590	MAPK10; PRKCZ	0.021	1.669	0.254
path:hsa04071	Sphingolipid signaling pathway	http://www.kegg.jp/kegg-bin/show_pathway?hsa04071/5602%09yellow/5590%09yellow	9.137	5602; 5590	MAPK10; PRKCZ	0.025	1.594	0.254
path:hsa05160	Hepatitis C	http://www.kegg.jp/kegg-bin/show_pathway?hsa05160/5602%09yellow/1364%09yellow	8.244	5602; 1364	MAPK10; CLDN4	0.031	1.514	0.254
path:hsa04068	FoxO signaling pathway	http://www.kegg.jp/kegg-bin/show_pathway?hsa04068/5602%09yellow/8471%09yellow	8.183	5602; 8471	MAPK10; IRS4	0.031	1.508	0.254
path:hsa04530	Tight junction	http://www.kegg.jp/kegg-bin/show_pathway?hsa04530/1364%09yellow/5590%09yellow	7.888	1364; 5590	CLDN4; PRKCZ	0.033	1.479	0.254